INTERNATIONAL JOURNAL OF OPTIMIZATION IN CIVIL ENGINEERING
Int. J. Optim. Civil Eng., 2012; 2(4):573-606

A STUDY ON NONLINEAR BEHAVIOR AND SEISMIC DAMAGE ASSESSMENT OF CONCRETE ARCH DAM-RESERVOIR-FOUNDATION SYSTEM USING ENDURANCE TIME ANALYSIS

M.A. Hariri Ardebili[a], H. Mirzabozorg[*, †,b] and R. Kianoush[c]
[a]*Department of Civil Environmental and Architectural Engineering, University of Colorado at Boulder, Boulder, Colorado, USA*
[b]*Department of Civil Engineering, K.N. Toosi University of Technology, Tehran, Iran*
[c]*Department of Civil and Environmental Engineering, Ryerson University, Toronto, Ontario, Canada*

ABSTRACT

In the present paper, nonlinear behavior of mass concrete simulated by smeared crack model is combined with Endurance Time Analysis (ETA) method for studying seismic response of arch dams. ETA is a time-history based dynamic pushover procedure in which special predesigned intensifying acceleration functions are used for analysis and estimation of structural responses in various performance levels by just a single analysis. For this purpose 203m DEZ arch dam is selected as case study and the finite element model of dam-reservoir-foundation system is excited in various performance levels. It was found that ETA provides reasonable responses in comparison with Time-History Analysis (THA) at equivalent target time. In addition, ETAleads to acceptable estimation of crack profiles within dam body and can reduce the total time of analyses, meaningfully. Generally, it was concluded that ETA can be considered as an alternative of THA in nonlinear analysis of arch dams.

Received: 5 May 2012; Accepted: 27 August 2012

KEY WORDS: endurance time analysis; smeared crack model; nonlinear seismic behavior; concrete arch dam; crack profile

[*]Corresponding author: H. Mirzabozorg Departmentof Civil Engineering, K.N. Toosi University of Technology, Tehran, Iran
[†]E-mail address: Mirzabozorg@kntu.ac.ir (H. Mirzabozorg)

1. INTRODUCTION

Among various types of dams, concrete arch dams have special position because not only little simple volume of material is used to close the valley, but also the shape of these dams reflects complicated technology in interaction between dam structure and its environment. Forces due to high water pressure applied on a thin concrete wall should be controlled by suitable method especially in high seismicity regions.

During recent years, design, construction and re-analysis of arch dams are one of important concerns in dam engineering society. Various methods for analysis of arch dams have been presented so far. For the first time in nineteen century some studies were done for design and analysis of simple arch dams. Theory of cylindrical thin wall structures with elastic behavior was one of these methods [1]. In this theory, stresses at each elevation are assumed to be the same as in a cylinder of equal outside radius. That is, water loads are resisted entirely by individual arch sections acting independently. Limitation of this method in double-curvature arch dams leads to invention of partly advanced methods such as trial load method [2]. The trial load method was based on the assumption that an arch dam is made of two horizontal and vertical structural members and water pressure is divided between arch and cantilever units in such away that the resulting arch and cantilever deflections and rotations at any point in the dam are equal [3]. Shortcomings of trial load method such as simple geometry and static analysis causes that finite element method is widely used in seismic design and analysis of arch dams. This method is able to take into account dynamic characteristics of ground motion and structure in behavior of arch dams. Two major branches of dynamic finite element method are finite-element Response Spectrum Analysis (RSA) and finite-element Time-History Analysis (THA).

The RSA uses earthquake response spectra as seismic input to compute maximum nodal displacement and element stress for each individual mode of vibration and then combines all significant modes to obtain total maximum response values [3]. In many cases RSA can create a good initial estimation of dam performance. But using mode super-position methods not only lead to some approximation in results but also is limited to use only in linear range of analysis. So it can be used only in moderate earthquakes level for evaluation of arch dams. Because this method provides only maximum value of responses, so it cannot be used alone for design purpose. THA method is able to capture both linear and nonlinear behavior of dams. In this method earthquake accelerograms are applied to dam-reservoir-foundation system as seismic input and time-history of any desired responses are plotted during excitation. THA method is the most accurate method in which characteristics like material nonlinearity, crack profile, reservoir and foundation effects and temperature variation can be considered during analysis for a certain accelerograms. On the other hand it has some disadvantages such as, responses depend on accelerogram especially in nonlinear analysis, so a set of accelerograms are required for analysis of an arch dam which is time consuming.

To overcome shortcomings in THA method, a new dynamic analysis technique was introduced recently called Endurance Time Analysis (ETA) method [4]. ETA is basically a time-history based dynamic pushover procedure which tries to predict responses of structures in various performance levels by subjecting them to a set of special predefined

intensifying excitations called as Endurance Time Acceleration Functions (ETAFs) [5]. The most surprising advantage of ETA method is how a simple analysis can be used instead of a large set of THAs with acceptable accuracy.

Application of ETA method in linear seismic analysis of structures has been studied before [6]. Validity and accuracy of this method in nonlinear seismic analysis of SDOF structures was investigated as well [5]. Application of ETA method in MDOF systems was studied similarly [7]. Estekanchi et al. [8] investigated the application of ETA method in seismic assessment of steel frames. Hariri et al. compared ability of the ETA and the THA in nonlinear analysis of steel moment resisting frames [9]. Valamanesh and Estekanchi studied the seismic behavior of the steel frames under multi-components excitations using the ETA method [10]. Alembagheri and Estekanchi studied seismic responses of on ground anchored and unanchored steel storage tanks using ETA method [11, 12 and 13]. They considered surface sloshing in numerical models and found that ETA is able to estimate conventional nonlinear response history with reasonable accuracy. Tavazo et al. [14] studied application of ETA for different types of shell structures in comparison with THA and RSA. Zeinoddini et al. [15] introduced Endurance Wave Analysis (EWA) method and its application for assessment of offshore structures under extreme waves. Valamaneshet al. [16] studied application of ETA in seismic analysis of concrete gravity dams. Hariri and Mirzabozorg [17] investigated accuracy of ETA for linear analysis of arch dam-reservoir-foundation systems. Also they evaluated seismic performance of arch dams using ETA and THA methods considering parameters like demand-capacity ratio and cumulative inelastic duration [18]. Hariri et al. [19] studied nonlinear behavior of arch dams considering contraction joints effects using ETA and THA methods.

In this paper, the ability of ETA method in estimating seismic response of arch dams and identifying probable damage within the dam body considering nonlinear behavior for mass concrete utilizing smeared crack approach is investigated. The concept of ETA method is first explained shortly and prospective methods to implement it are discussed. Parallel with ETA, THA is conducted to compare the results obtained from the two methods. For this purpose DEZ double curvature arch dam is selected as case study. Fluid-Structure Interaction (FSI) effect of reservoir water is considered by modelling water as compressible material. Moreover foundation rock is modelled as a mass-less medium and finite element model of the system is excited in various performance levels using accelerograms and also ETAFs.

2. FUNDAMENTALS OF ONE-COMPONENT ETA

ETA method is a time-history based dynamic pushover procedure used in seismic analysis and performance evaluation of structures by measuring their resilience when they are subjected to ETAFs [5, 18]. In this method, numerical or experimental model of structures are subjected to intensifying ETAFs and structural responses, such as displacements and stresses are recorded during the analysis up to the point where the structure collapses or the analysis is terminated. Then behavior of the structure can be observed at target time which is calculated using design response spectrum. It is noteworthy that in this method time is corresponding with intensity and longer target time for a certain structure means that it

should endure stronger dynamic excitation.

If this test is utilized for two frames with unknown properties, the longer endurance time which is time duration from start of the test or analysis to collapse or target point, is interpreted as better performance of that frame [20].Figure 1 displays schematically methodology of analyzing arch dams based on ETA method in the present paper. In this approach after preparing appropriate 3D finite element model of dam-reservoir-foundation, the system is excited using an ETAF in Upstream/Downstream (US/DS) direction, which is the major direction of excitation in arch dams. It should be mentioned that, although some investigations have been conducted for developing ETA method for the cases with two and three components excitations, there is not still any established methodology for multi components analyses of structures using this method. In the next step, the equivalent target time is calculated for each performance level using ETAFs and the desired performance level response spectrum. Various responses of the dam at equivalent target time describe behavior of the dam in a certain performance level. For example until $t = t_1$ in which the structure is required to safely withstand with limited repairable damage, the performance level is evaluated as Design Base Level (DBL) and t_1 is called as t_{eq}(DBL), until $t = t_2$ in which some cracks are propagated within the dam body but are discrete and repairable, the performance level is evaluated as Maximum Design Level (MDL) and t_2 is called as t_{eq}(MDL) and finally until $t = t_3$ where extensive damage is observed within the dam body and continuous cracks are revealed on US and DS faces which are not repairable, the performance level is evaluated as Maximum Credible Level (MCL) and t_3 is called as t_{eq}(MCL) [18].

It is worth noting that for obtaining the extreme results in analyzing the system utilizing THA or ETA methods, seismic excitation should be applied to the system in two opposite directions to obtain the most critical direction that would cause the largest structural response. For one-component excitation a total of two permutations are required which are shown as +US/DS and -US/DS in which (+) and (-) signs indicate that earthquake record is multiplied by +1 (zero phase) or -1 (180 phase) to account for the most unfavorable earthquake direction [21].

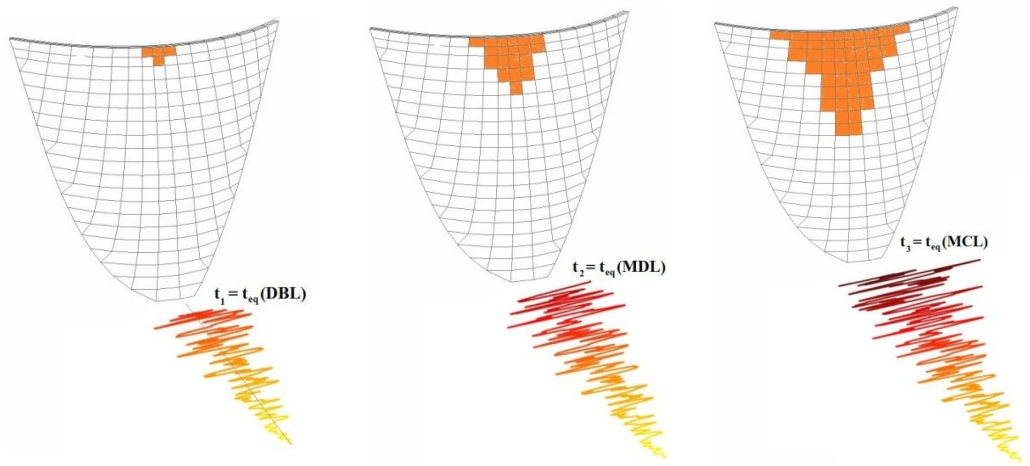

Figure 1. Arch dam damage profile in various performance levels using ETAF

The first generation of acceleration functions was produced using random numbers with a Gaussian distribution of zero mean and a variance of unity [4, 22]. In this method, stimulator function is defined as a finite sum of harmonic functions as:

$$a(t) = \sum_{i=1}^{N} A_i . \sin(\omega_i t + \phi_i) \tag{1}$$

Where *a(t)* is acceleration function, N is number of acceleration points, ω_i is angular frequency of term *i*, φ_i is angle of phase delay in sinusoidal component and A_i is Fourier amplitude. If amplitudes and angle of phase delay in sinusoidal component supposed as vector form, it is possible to generate different functions by constant amplitude and fluctuating angle of phase delay. All generated functions produced by this method are stationary and ergodic. A stationary random acceleration function was generated using $\delta t = 0.01$ and $n = 2^{11} = 2048$ with PGA = 1g. So duration of the acceleration function was equal to $\delta t \times n = 20.48$ s.

The frequency content of the random acceleration functions that was statistically similar to a white noise was then modified, in order to resemble real earthquake accelerograms. For this purpose, filter functions were applied to the random acceleration functions as explained by Clough and Penzien [22]. The frequency content was then further modified in order to generate acceleration functions with response spectra that are compatible with typical seismic code response. For this purpose, the response spectra of the Iranian National Building Code (INBC) [23] had been used as a sample. In the next step, the acceleration values were adjusted for target values of velocity and acceleration (which in this case were set to zero). Finally, the acceleration values were multiplied in a density function ($g(t)$=t/10). Three acceleration functions had been generated and named as acc1, acc2 and acc3.The term “first generation” is predicated to acc1-3 acceleration functions because they generated using a heuristic approach without direct control over response parameters.

In order to improving general characteristics of acceleration functions and using them in structural engineering, second generation of ETAFs was produced [24]. In this generation, in order for the ETAFs to somehowcorrespond to average code compliant design level earthquakes,the concept of the response spectrum has been more directlyinvolved. Like as first generation, linear intensifying pattern was chosen for this set anddesigned in such a way as to produce dynamic responses equalto the code’s design spectrum at a predefined time, $t_{eq\bullet}$.In this way, the target spectral acceleration and displacement are defined as follow [6]:

$$\begin{aligned} S_a^{ET}(t,T) &= \frac{t}{t_{eq\bullet}} S_a^{TARGET}(T) \\ S_u^{ET}(t,T) &= \frac{t}{t_{eq\bullet}} S_a^{TARGET}(T) \times \frac{T^2}{4\pi^2} \end{aligned} \tag{2}$$

where $S_a^{ET}(t,T)$ and $S_u^{ET}(t,T)$ are ETAFs target acceleration and displacement response

values at time t, $S_a^{TARGET}(T)$ is target acceleration responses of structure and T is period of free vibration. Considering that analytical approach to finding an ETAF that satisfies Eq. (2) is formidably complicated, so numerical optimization technique was used to solve it by following formulation [25]:

$$\underbrace{\min}_{a_g} F(a_g) = \int_0^{T_{max}} \int_0^{t_{max}} \left\{ \left[S_a^{ET}(t,T) - S_a(t,T) \right]^2 + \alpha \left[S_u^{ET}(t,T) - S_u(t,T) \right]^2 \right\} dt dT \qquad (3)$$

Where a_g is the acceleration function being sought and α is a weighting parameter. Starting from a randomly generated acceleration function, unconstrained optimization can be used to solve the problem. The three ETAFs that have been generated by this method are called as ETA20a01-03 (a-series). A typical ETAF from this set and also average response spectrum of this set at various times are depicted in Figure 2. It is worthy nothing that the base target time has been assumed 10s in generation of this set, i.e. the ETAFs response spectrum reaches the standard code level at t = 10s.

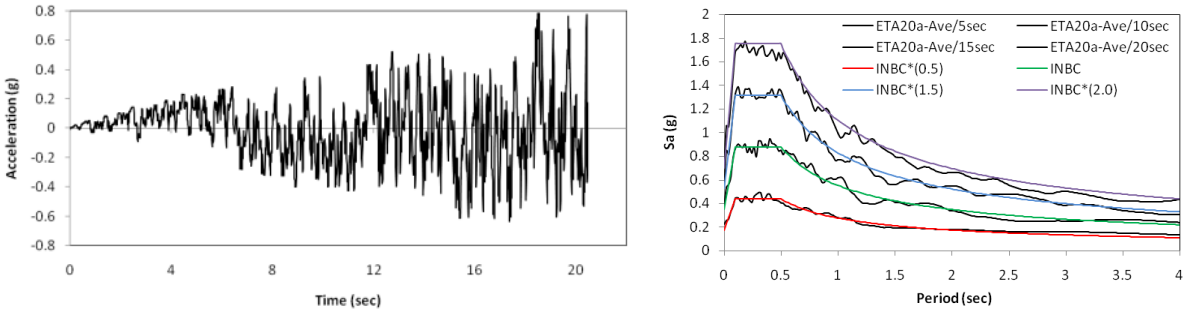

Figure 2. Typical acceleration function and average response spectrum of a-series at various times

To investigate potential of ETA method in comparison with THA, a set of ETAFs called as ETA20e01-03 was used in present paper. This set that is also called e-series and entitled as ETA20e01-03 consists three ETAFs generated in such a way that their intensity, PGA and response spectra increase by the time. To reach this goal, 20 accelerograms which were defined by the NEHRP and used in FEMA 440, were selected as base ground motions. From these ground motions, 7 records whose response spectra shapes were more compatible with the response spectrum of soil type II of INBC were selected (Table 1). These 7 accelerograms which are called as GM1 set were scaled to produce a response spectrum that is compatible with the INBC spectrum. Finally, the average of the pseudo acceleration spectrum of these scaled accelerograms is obtained and smoothed. The smoothed spectrum was used as the base target spectrum in generating this set of ETAFs. These ETAFs are generated in such a way that their response spectra increase by the time, hence response of the structure under this kind of accelerograms gradually increases with time. A typical ETAF is depicted in Figure 3. Also, corresponding PGA is shown in this figure at various times. As it is obvious, PGA increase inalmost linear trend with time passage. Figure 3

alsopresents response spectrum of average of ETAFs (e-series) at various times. This set has been generated in a manner that its response spectrum atthe base target time which is taken to be 10s is compatible with the base target response spectrum used for generation of e-series (GM1 set) [18, 24].

Table 1. Characteristics of GM1 set of ground motions

Ground motion	Station No.	Component	Magnitude (Ms)	PGA (cm/s^2)
Landers (06/28/1992)	12149	0	7.5	167.8
Loma Prieta (10/17/1989)	58065	0	7.1	494.5
Loma Prieta (10/17/1989)	47006	67	7.1	349.1
Loma Prieta (10/17/1989)	58135	360	7.1	433.1
Loma Prieta (10/17/1989)	1652	270	7.1	239.4
Morgan Hill (04/24/1984)	57383	90	6.1	280.4
North-Ridge (01/17/1994)	24278	360	6.8	504.2

It is worthy to note that ETA response spectrum remains linearly proportional to the target spectrum in any lapse of time. For example response spectrum for average of ETAFs at time t=10s is twice of the response spectrum at time t=5s and half of that at time t=20s (Figure 3) [17].

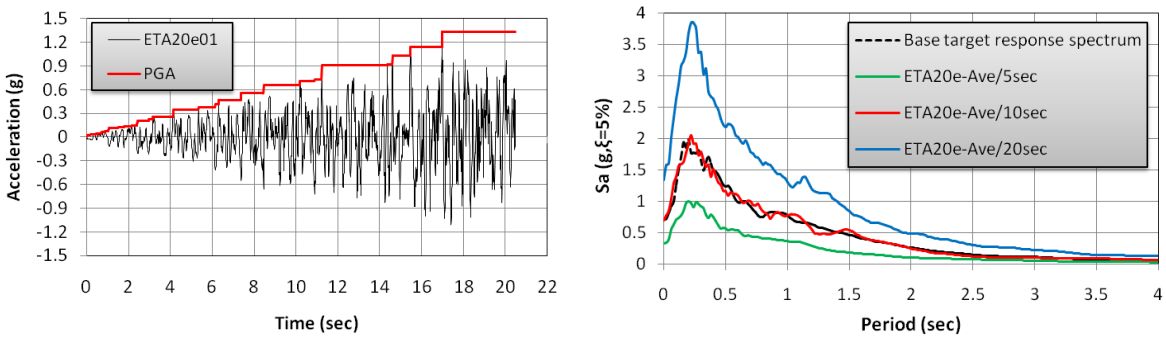

Figure 3. A typical ETAF, corresponding PGA and average response spectrum from e-series at various times

3. NUMERICAL MODELING OF A HIGH ARCH DAM

DEZ double curvature arch dam in Iran was selected as case study. Crest length is 240m and thickness at the crest level is 4.5m. Finite element idealization prepared for the dam, foundation rock and reservoir is shown in Figure 4, which consists of 792 solid elements for

modeling dam and concrete saddle, 3770 solid elements for simulation of foundation rock and 3660 fluid elements in reservoir domain. Material property of mass concrete and foundation rock are presented in Table 2. In addition, reservoir water density is assumed 1000kg/m^3, sound velocity is 1440m/s in water and wave reflection coefficient for reservoir around boundary is supposed 0.8, conservatively.

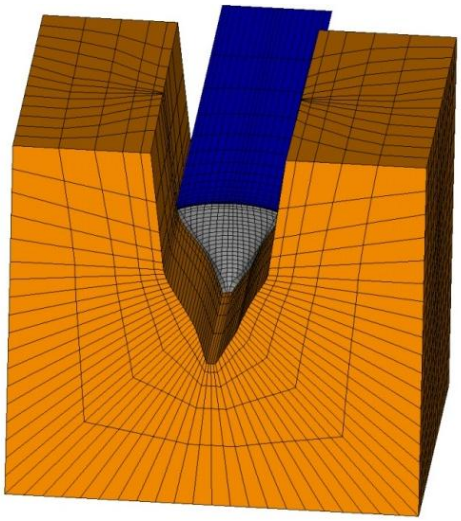

Figure 4. Finite element model of dam, foundation rock and reservoir

Table 2. Material property of mass concrete and rock

		Static condition	**Dynamic condition**
Mass Concrete	Isotropic Elasticity	40GPa	46GPa
	Poisson's Ratio	0.2	0.14
	Density	2400kg/m^3	2400kg/m^3
	Uni-axial Compressive Strength	$(f_c)_{static}$ = 35MPa	$(f_c)_{dynamic}$ =36.5MPa
	Uni-axial tensile Strength	$(f_t)_{static}$ = 3.4MPa	$(f_t)_{dynamic}$ = 5.1MPa
Foundation	Isotropic Elasticity-Saturated	13GPa	13GPa
	Isotropic Elasticity-Unsaturated	15GPa	15GPa
	Poisson's Ratio	0.25	0.25

4. LOADING

Applied loads on the system are dam body self-weight, hydrostatic pressure in Normal Water Level and seismic load. In addition, thermal load corresponding to summer condition

is applied on the dam body. It is worthy to note that thermal load applied on the structure has been extracted from calibrated thermal transient analyses conducted using real data at the dam site taking into account solar radiation on exposed surfaces of the dam body [26].

The system is excited at foundation boundaries using ETAFs and scaled earthquake records and β-Newmark method is utilized to solve the coupled nonlinear problem of dam-reservoir-foundation model. Moreover structural damping is taken to be 5% of critical damping. It should be remembered that all seismic inputs are exerted to the system in only one major direction which is Upstream/Downstream (US/DS) direction. Although seismic analysis of concrete arch dams should be utilized considering appropriate three-component ground motion records (or any multi-directional seismic input), in present paper for the first time, ETA and THA methods were compared in evaluation of arch dams considering only one major direction of seismic input which is US/DS direction. Although using one-component ground motion instead of three-component one reduces results obtained from analysis of coupled system, it has no effect in general methodology. In multi-component analysis of structures based on ETA method it is just needed that ETAFs be scaled based on horizontal and vertical design response spectrums and suitable reduction factor be used for second horizontal component as described in [10, 27].

4.1. Accelerograms for THA

Based on ICOLD 1989 [28] three performance levels must be considered for seismic design and evaluation of dam-reservoir-foundation system that are DBL, MDL and MCL (as mentioned before). Based on seismic hazard analysis of the dam site, design spectrum for three performance levels are extracted considering ξ=5% as shown in Figure 5 [29, 30]. Figure 6 shows horizontal components of accelerograms in various performance levels which are selected based on source characteristics, source-to-site transmission path properties, and site conditions.

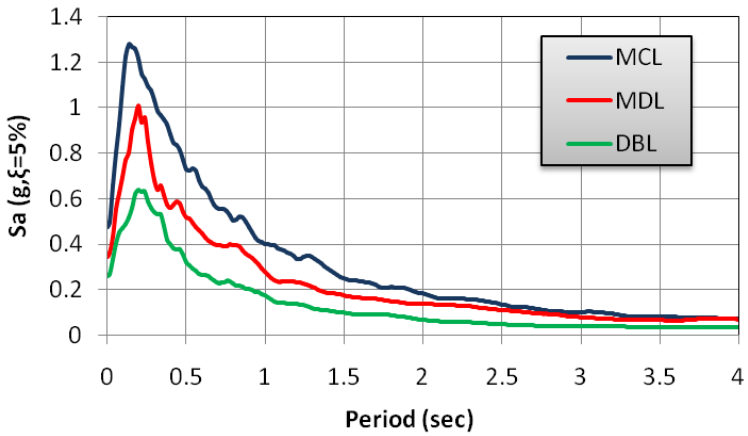

Figure 5. Response spectrum of three seismic performance levels

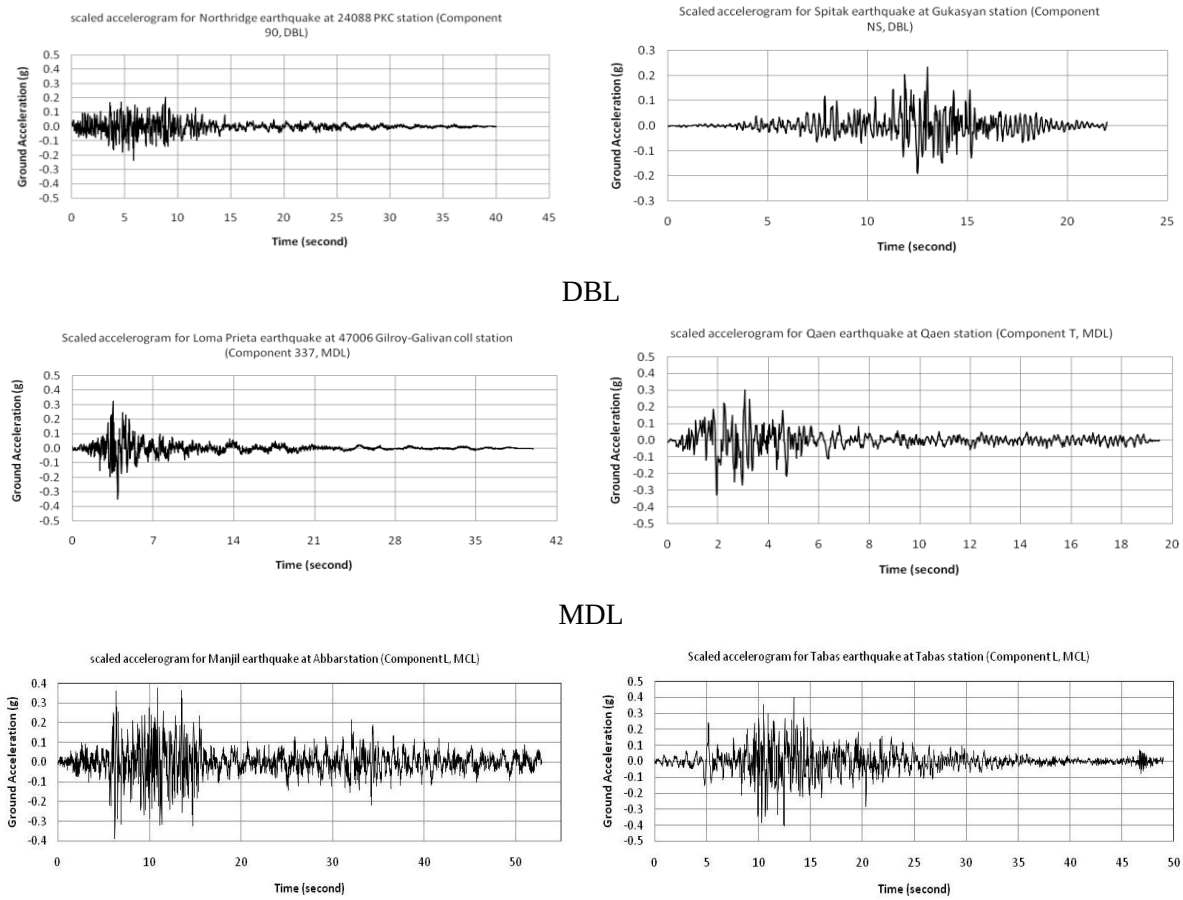

Figure 6. Horizontal components of accelerograms in various performance levels

5. MODAL ANALYSIS AND CALCULATION OF EQUIVALENT TARGET TIME

Response of the dam in each time window is corresponding with a certain performance level. Ordinary low target times are corresponding with low performance levels and vice versa. Generally there are two approaches in calculation of equivalent target time, i.e. methods based on concept of spectrum analysis and statistical methods [17].In the present study, statistical methods are used for determining appropriate equivalent target time which is suitable for nonlinear analyses. In the proposed technique at the current study, 10^{th} second of ETAFs is selected as base target time and therefore, the average response spectrum resulted up to the 10^{th} second of ETAFs is interpreted as base response spectrum (which is corresponding with base target response spectrum for generation of ETAFs).

Consequently, equivalent target time for various performance levels is calculated by multiplying ETAF base response spectrum with factor ψ, called spectrum ratio, in the manner that the surface enclosed between the two curves of $\psi \times S_a^{ET}$ and S_a^{TR} (which is the

desired performance level response spectrum) taking into account percentage of the effective mass at each period is set to zero (concept of energy method). The period interval in previous step is selected in a manner that includes more than 90% of total mass of the system. After determining ψ (with trial and error technique), the equivalent target time for the desired performance level is given as:

$$t_{eq}(T_R) = \psi(T_R) \cdot t_{eq\bullet} \tag{4}$$

in which $t_{eq\bullet}$ is base target time taken to be 10s and $\psi(T_R)$ is spectrum ratio for the desired performance level with return period T_R. The above procedure can be represented mathematically as following:

$$\min \left| \left\{ \sum_{T_1}^{T_2} (m_{eff}^{i}) \left[(\psi_{III}).(S_a{}^{ET,i}) - (S_a{}^{T_R,i}) \right] \right\} \right| \quad , \quad i \in [T_1, T_2] \tag{5}$$

in which $S_a{}^{T_R,i}$ and $S_a{}^{ET,i}$ are spectral accelerations in i^{th} mode and $[T_1, T_2]$ is period interval including 90% of total mass of the system, m_{eff}^{i} is effective mass of the system in excitation direction in i^{th} mode, i is any effective mode and subscript III is referred to the explained method in the present paper which is based on arithmetic mean weight concept. Figure 7 shows schematically determination of spectrum ratio for MCL. As can be seen, the surface enclosed between $S_a{}^{MCL}$ and $S_a{}^{ET} \times 0.636$ considering the effective mass of each mode in period interval [0.04s, 0.48s], which includes 94.25% of total mass of the dam-reservoir-foundation system is approximately zero. In the second step, equivalent target time for MCL can be obtained by multiplying 0.636 in 10s (base target time), which is 6.36s. It means that the results obtained from average ETAs up to 6.36s should have the same or close values to the average maximum values resulted from THAs in MCL. This rule is indefeasible in other performance levels. Based on analyses conducted by the authors, spectrum ratio and equivalent target times for various performance levels are given as in Table 3.

Table 3. Spectrum ratio and equivalent target time for three performance levels

Spectrum Ratio	**Equivalent Target Time**
$\psi_{III}(MCL) = 0.636$	$t_{eq\,III}(MCL) = 6.36\,\mathrm{s}$
$\psi_{III}(MDL) = 0.417$	$t_{eq\,III}(MDL) = 4.17\,\mathrm{s}$
$\psi_{III}(DBL) = 0.325$	$t_{eq\,III}(DBL) = 3.25\,\mathrm{s}$

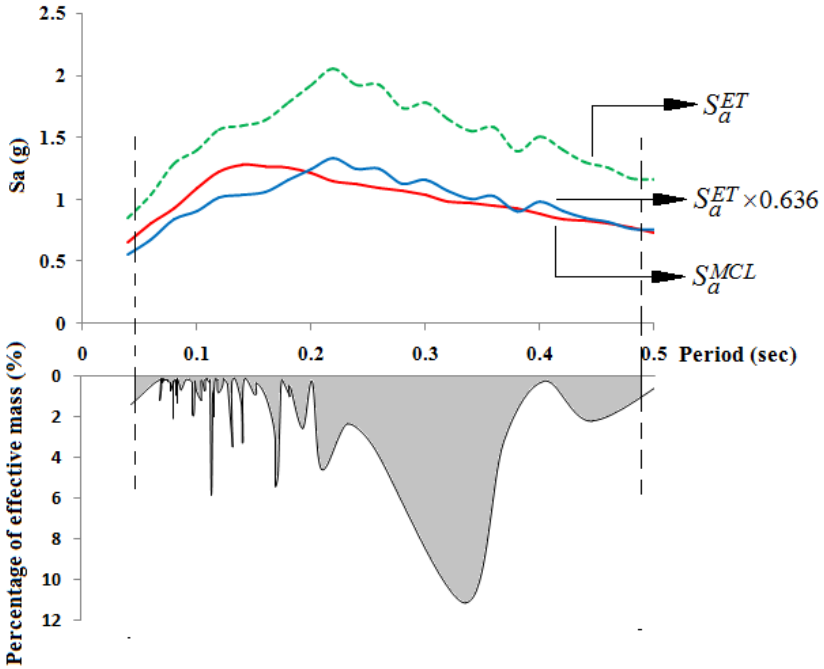

Figure 7. Determining equivalent target time based on heuristic statistical method (concept of arithmetic mean weight and energy method)

6. SMEARED CRACKAPPROACH FORMASS CONCRETE

Nonlinear behavior of arch dams originates from joint and material nonlinearity. In the present paper, material nonlinearity is considered for conducting ETA and THA which is based on smeared crack model. It is worthy to note that based on authors experience, general pattern of crack profiles are the same for the models with and without joint nonlinearity. However, there are differences in damaged areas extensions when joints are modelled between dam blocks. Anyway, the main object of the present paper is investigating ability of ETA method in estimating seismic behavior of high arch dams.

After initiation of fracture process, determined by a suitable constitutive model, the pre-crack material stress-strain relation is replaced by an orthotropic relation with material reference axis system aligned with the fracture direction. The tension stiffness across the crack plane is either eliminated suddenly or a gradual stress-release criterion is applied. Thus, only the constitutive relation is updated with propagation of cracks and the finite element mesh is kept unchanged [31]. The main advantage of the model lies in its simplicity and cost effectiveness, although the physical nature of crack representation is questionable [32].

In the utilized model, it is assumed that concrete material is initially (before cracking) isotropic and linear. The stress-strain matrix is defined by the Eqn.6 given as [31, 33]:

$$[D_{linear}] = \frac{E}{(1+v)(1-2v)} \begin{bmatrix} (1-v) & v & v & 0 & 0 & 0 \\ v & (1-v) & v & 0 & 0 & 0 \\ v & v & (1-v) & 0 & 0 & 0 \\ 0 & 0 & 0 & \frac{1-2v}{2} & 0 & 0 \\ 0 & 0 & 0 & 0 & \frac{1-2v}{2} & 0 \\ 0 & 0 & 0 & 0 & 0 & \frac{1-2v}{2} \end{bmatrix} \quad (6)$$

where, E is isotropic Young's modulus for concrete and v is Poisson's ratio. In concrete, cracking occurs when the principal tensile stress in any direction lies outside the failure surface. Cracking is permitted in three orthogonal directions at each integration point. When cracking occurs at an integration point, the stress-strain relation is modified by defining a weak plane normal to the crack direction, which is unable to endure any tensile stresses. The presence of crack at an integration point and in special direction, represent through modification of stiffens matrix by exerting shear transfer coefficient in cracked plane.

Based on the fact that concrete has been cracked in one, two or three orthogonal directions, the stiffness matrix can be represented in following forms:

I) Concrete has been cracked in one direction and the crack is open:

$$[D_{cracked}^{open}] = \frac{E}{1+v} \begin{bmatrix} \frac{E^S(1+v)}{E} & 0 & 0 & 0 & 0 & 0 \\ 0 & \frac{1}{1-v} & \frac{v}{1-v} & 0 & 0 & 0 \\ 0 & \frac{v}{1-v} & \frac{1}{1-v} & 0 & 0 & 0 \\ 0 & 0 & 0 & \frac{\beta_{open}}{2} & 0 & 0 \\ 0 & 0 & 0 & 0 & \frac{1}{2} & 0 \\ 0 & 0 & 0 & 0 & 0 & \frac{\beta_{open}}{2} \end{bmatrix} \quad (7)$$

Where E_s is the secant modulus of elasticity, υ is Poisson's ratio and β_{open} is open shear transfer coefficient and defined as the factor that represents shear strength reduction across the cracked face.

II) Concrete has been cracked in one direction and the crack is closed:

$$[D_{cracked}^{closed}] = \frac{E}{(1+v)(1-2v)} \begin{bmatrix} (1-v) & v & v & 0 & 0 & 0 \\ v & (1-v) & v & 0 & 0 & 0 \\ v & v & (1-v) & 0 & 0 & 0 \\ 0 & 0 & 0 & \frac{\beta_{close}(1-2v)}{2} & 0 & 0 \\ 0 & 0 & 0 & 0 & \frac{1-2v}{2} & 0 \\ 0 & 0 & 0 & 0 & 0 & \frac{\beta_{close}(1-2v)}{2} \end{bmatrix} \quad (8)$$

Where $_{close}$ is closed shear transfer coefficient. The shear transfer coefficient, β, represents conditions of the crack face. The value of β ranges from 0.0 to 1.0, with 0.0 representing smooth crack (complete loss of shear transfer) and 1.0 representing a rough crack (no loss of shear transfer).

III) Concrete has been cracked in two directions and the cracks are open:

$$[D_{cracked}^{open}] = E\begin{bmatrix} \frac{E^S}{E} & 0 & 0 & 0 & 0 & 0 \\ 0 & \frac{E^S}{E} & 0 & 0 & 0 & 0 \\ 0 & 0 & 1 & 0 & 0 & 0 \\ 0 & 0 & 0 & \frac{\beta_{open}}{2(1+\nu)} & 0 & 0 \\ 0 & 0 & 0 & 0 & \frac{\beta_{open}}{1(1+\nu)} & 0 \\ 0 & 0 & 0 & 0 & 0 & \frac{\beta_{open}}{2(1+\nu)} \end{bmatrix} \tag{9}$$

IV) Concrete has been cracked in two directions and both cracks are closed:

$$[D_{cracked}^{closed}] = \frac{E}{(1+\nu)(1-2\nu)}\begin{bmatrix} (1-\nu) & \nu & \nu & 0 & 0 & 0 \\ \nu & (1-\nu) & \nu & 0 & 0 & 0 \\ \nu & \nu & (1-\nu) & 0 & 0 & 0 \\ 0 & 0 & 0 & \frac{\beta_{close}(1-2\nu)}{2} & 0 & 0 \\ 0 & 0 & 0 & 0 & \frac{(1-2\nu)}{2} & 0 \\ 0 & 0 & 0 & 0 & 0 & \frac{\beta_{close}(1-2\nu)}{2} \end{bmatrix} \tag{10}$$

V) Concrete has been cracked in three directions and the cracks are open:

$$[D_{cracked}^{open}] = E\begin{bmatrix} \frac{E^S}{E} & 0 & 0 & 0 & 0 & 0 \\ 0 & \frac{E^S}{E} & 0 & 0 & 0 & 0 \\ 0 & 0 & 1 & 0 & 0 & 0 \\ 0 & 0 & 0 & \frac{\beta_{open}}{2(1+\nu)} & 0 & 0 \\ 0 & 0 & 0 & 0 & \frac{\beta_{open}}{2(1+\nu)} & 0 \\ 0 & 0 & 0 & 0 & 0 & \frac{\beta_{open}}{2(1+\nu)} \end{bmatrix} \tag{11}$$

VI) Concrete has been cracked in three directions and all cracks are closed. In this situation Eqn.10 can be written again. It must be noted that all above stress-strain relations are written in local coordinate system that is parallel to principal stress directions.

7. RESULTS AND DISCUSSION

In the following subsections, ability of ETA method in estimating various parameters such as displacement, velocity, acceleration and stress is considered. Obviously, parameters like velocity and acceleration at the crest are not utilized directly for seismic safety evaluation of concrete arch dams. However, investigation on these parameters can be valuable mathematically.

7.1. Displacement

In this section, displacements obtained from ETA method at target time and THAs are compared with each other along upstream nodes of the crown cantilever. Figure 8 shows non-concurrent envelopes of displacement along height of crown cantilever extracted from THA and ETA method in various performance levels. Also figure 9 displays percentage of errors between average of THA results and ETAFs in a certain performance level along height of the block.

As is evident, using three ETAFs and taking their average increase compatibility of ETA method with average of THA. In DBL, there is great compatibility between the results of ETA method and THA. The maximum percentage of error in this performance level is limited to 5% at crest of the dam. In upper half of central cantilever ETA overestimates the results. It means that the equivalent target time for DBL is little more than its real value. In MDL, some differences are observed in upper 1/3 part of the central cantilever. It must be noted that based on performance evaluation of the dam by linear analysis [17] an area with nonlinear behavior and probably damaged waspredicted in upper part of the body in vicinity of the crest causing different behavior at this region. Anyway, errors in this performance level are more than DBL and limited to 11% at the crest point. Like as DBL, ETA overestimates results of displacements in MDL.

In MCL, high nonlinear behavior is observed in upper ¼ part of the dam. So displacements increase from about 60mm in MDL to about 110mm in MCL at the crest point. Errors are limited to 12% in this level and in spite of the two previous levels, ETA underestimates the results and it seems that 6.36s as equivalent target time in MCL is less than its real value.

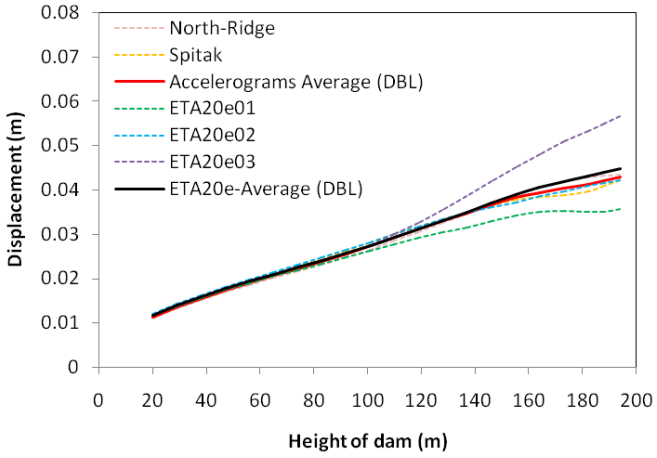

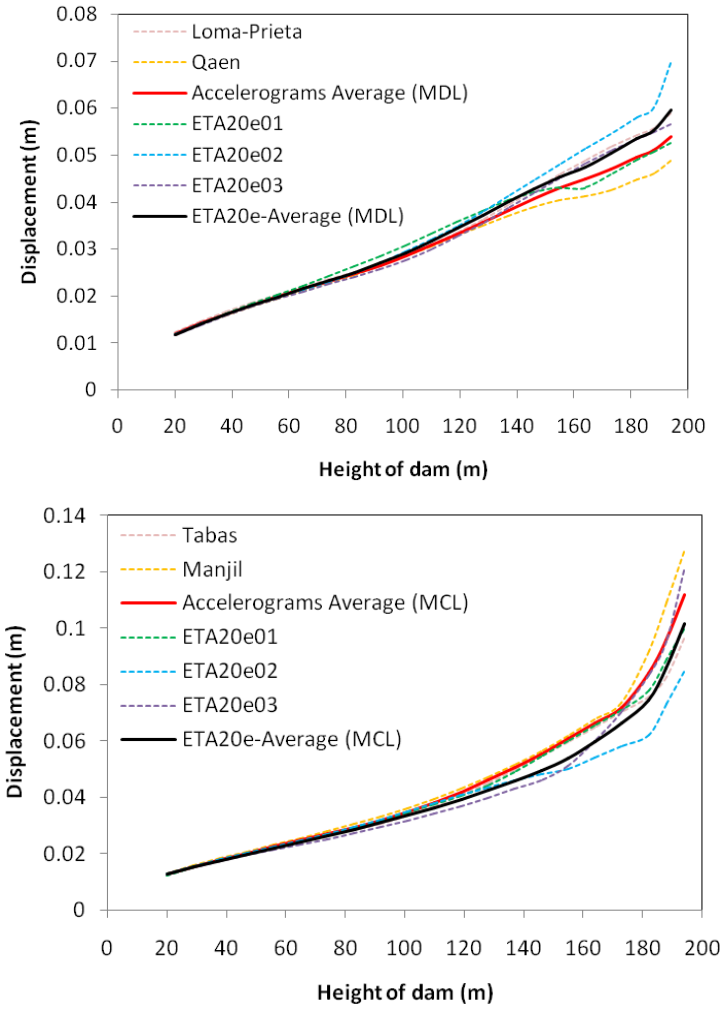

Figure 8. Non-concurrent envelopes of displacement along central cantilever in various performance levels

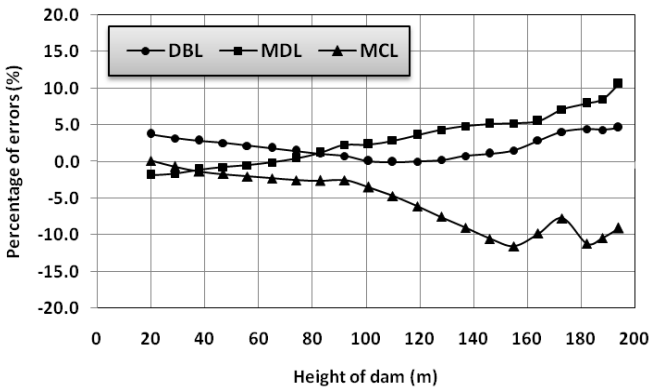

Figure 9. Percentage of errors between average of THAs and ETAFs in three performance levels for displacement

7.2. Velocity

Figure 10 shows non-concurrent envelopes of velocity along height of crown cantilever extracted from THAs and ETA in various performance levels. Also figure 11 displays percentage of errors between average of THAs results and ETAFs in a certain performance level along the height. In DBL, ETA gives good estimation of velocities, because in lower ¾ part of dam the results of ETA fluctuate around the THA results. Although some high errors are observed in central 1/3 part of the dam in MDL, similarity of ETA and THA is acceptable in this level. Contrary to expectation, in MCL percentage of errors are about zero in lower half part of the dam and are limited to 18% in upper half part. Finally, like as displacement, ETA overestimates results in DBL and MDL and underestimates them in MCL.

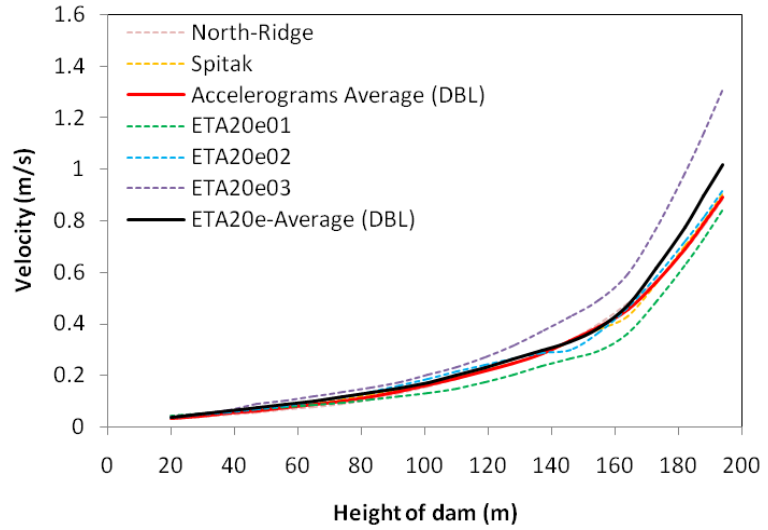

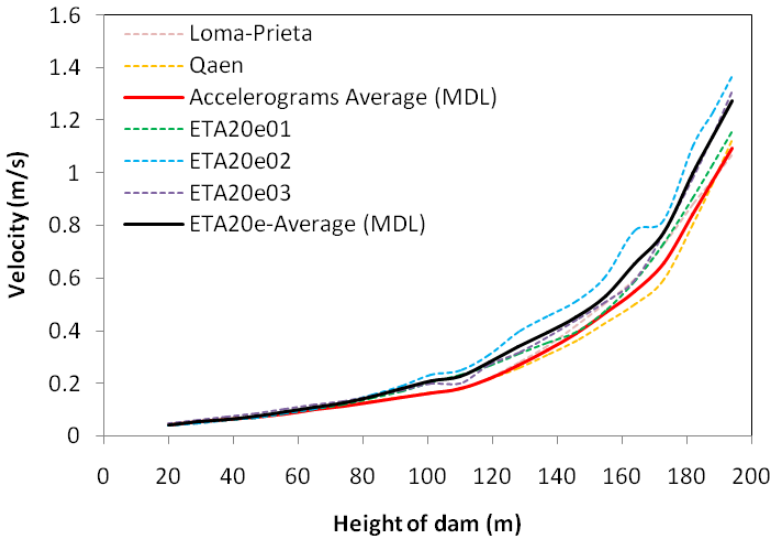

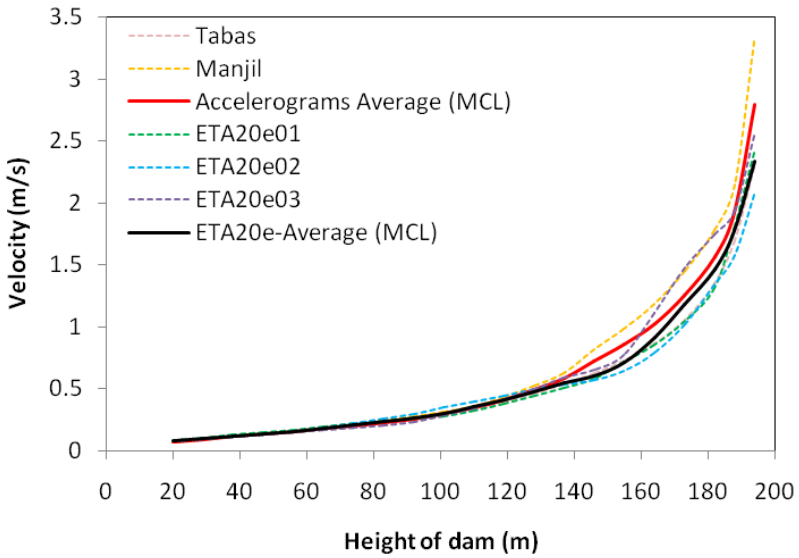

Figure 10. Non-concurrent envelopes of velocity along central cantilever in various performance levels

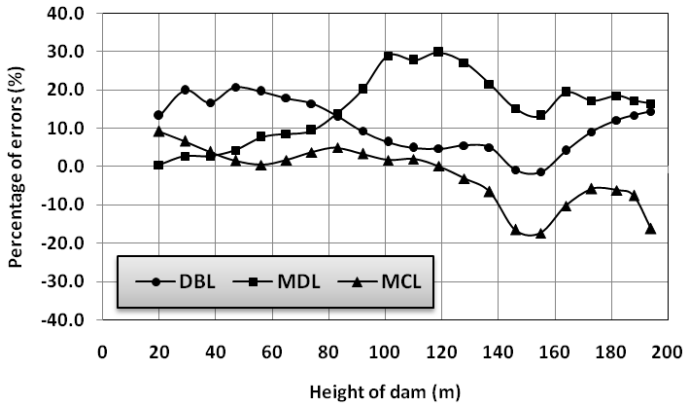

Figure 11. Percentage of errors between average of THAs results and ETAFs in three performance levels for velocity

7.3. Acceleration

Figure 12 shows non-concurrent envelopes of acceleration along the height of crown cantilever extracted from THAs and ETA in various performance levels. Also figure 13 displays percentage of errors between results obtained from average of THAs and ETAFs in a certain performance level along the height of the block. In DBL and MDL in which the nonlinearity of the system is low or moderate, values obtained from both ETA and THAs are acceptable. In both levels ETA overestimates results but percentages of errors are limited to 20%. In MCL, because of extensive damage in upper ¼ part of the dam, motions with very high acceleration (which is sign of uncontrolled motion called as projectile-motion) are observed in this part and percentage of errors along cantilever shows

considerable variation. Anyway, in this performance level ETA gives acceptable prediction of THA results.

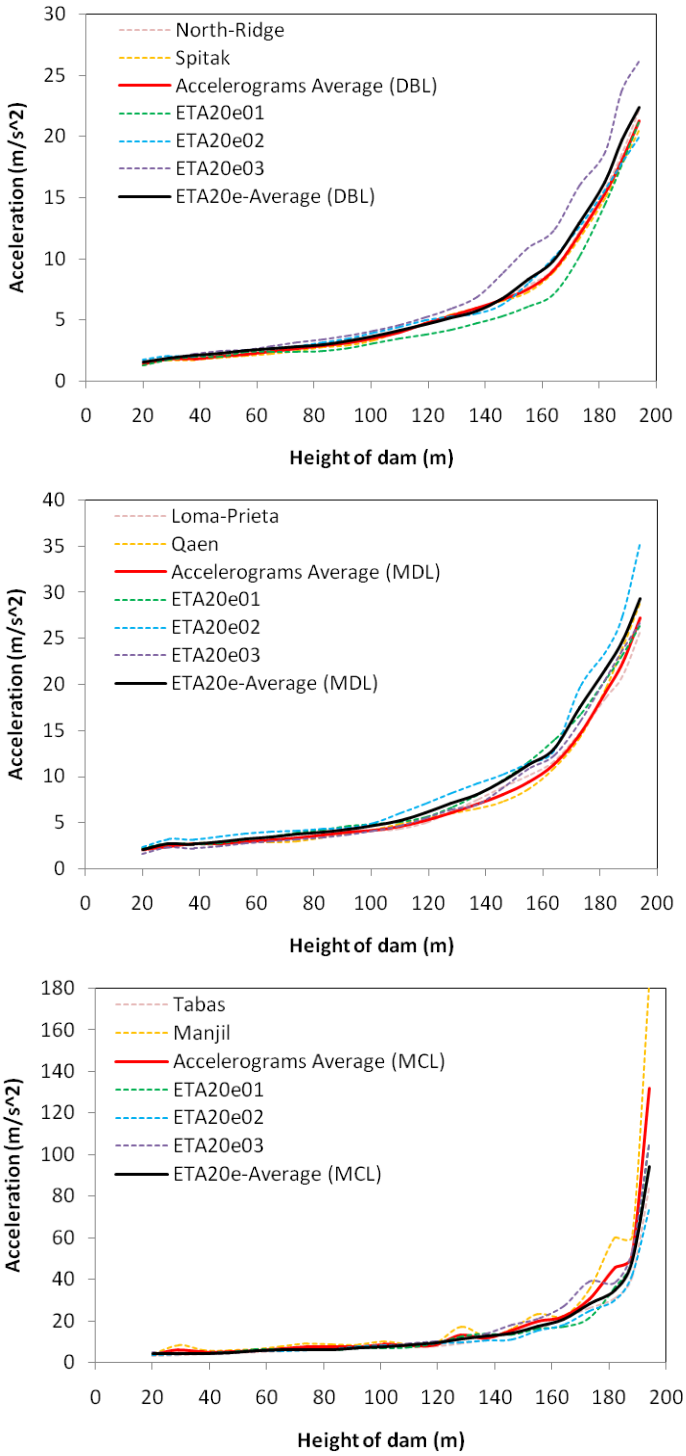

Figure 12. Non-concurrent envelopes of acceleration along central cantilever in various performance levels

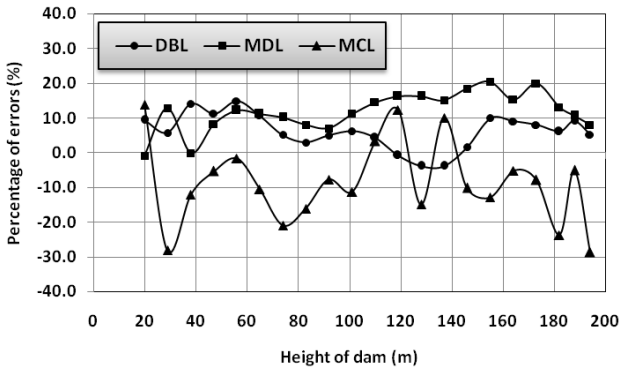

Figure 13. Percentage of errors between average of THAs results and ETAFs in three performance levels for acceleration

7.4. Principal stresses

Figure 14 shows non-concurrent envelopes of principal stresses along height of central cantilever extracted from THAs and ETA in various performance levels. In all cases first principal stress (S1) is limited to dynamic tensile stress of mass concrete. Generally, the correspondence between average of THAs results and ETAFs is better in low excitation levels. Because crushing is not considered in the present study, third principal stress (S3) increases for various nodes along cantilever with rise of excitation level. Percentage of errors between ETA and THAs results for S3 is lower than S1 and there is good similarity between two methods in all performance levels.

Figures 15 to 20 display average non-concurrent envelopes of principal stresses extracted from THAs and ETAFs on upstream and downstream faces of the dam body in various excitation levels. As can be seen, there is excellent similarity between envelopes in DBL. Although similarity of S1 envelopes in MDL is very great, some minor differences are shown in upper central part on upstream face. In MCL, S3 envelopes extracted from average of ETA and THA are approximately the same. However differences are appear in stress distribution pattern on US and DS faces for S1.

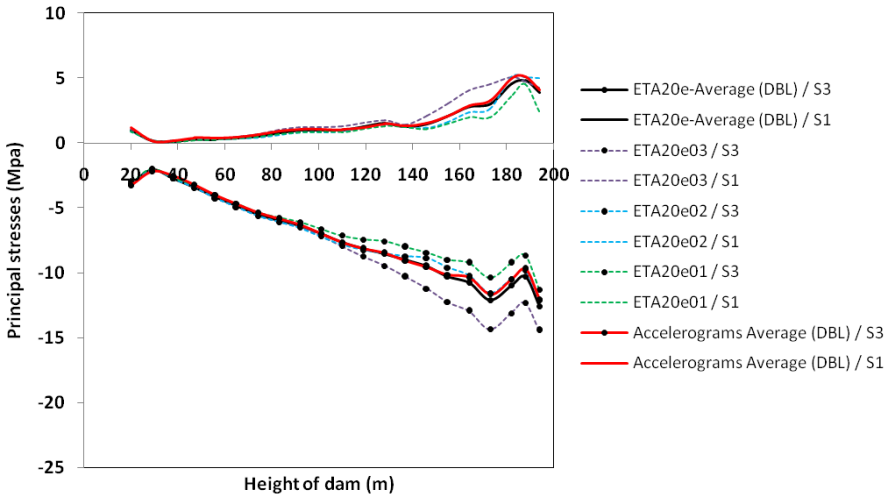

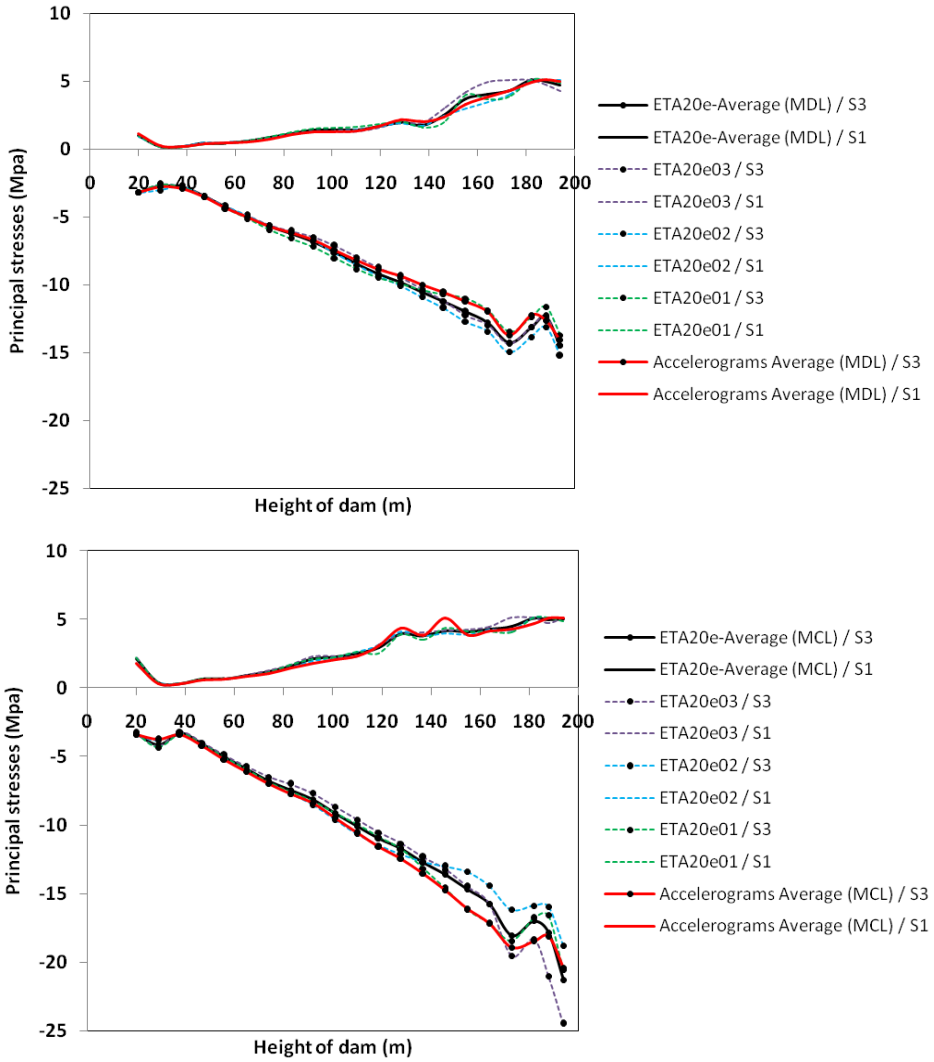

Figure 14. Non-concurrent envelopes of principal stresses along central cantilever in various performance levels

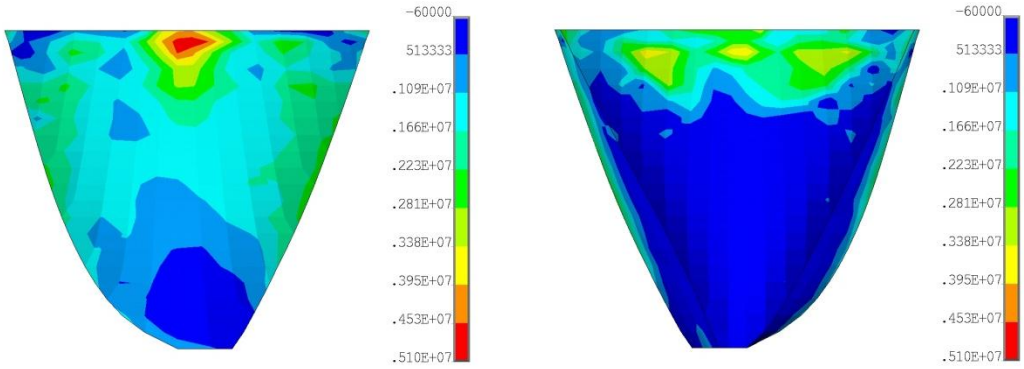

ETA20e-Average (DBL)

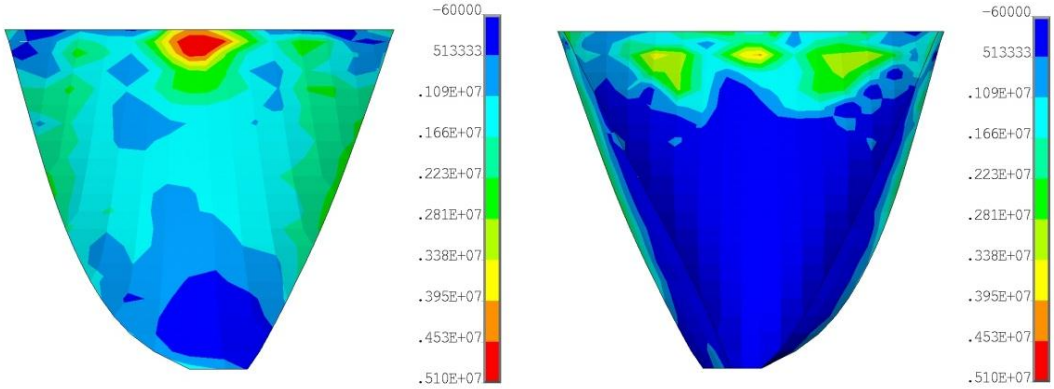

Accelerograms Average (DBL)

Figure 15. Average non-concurrent envelopes of S1 on US and DS faces; DBL

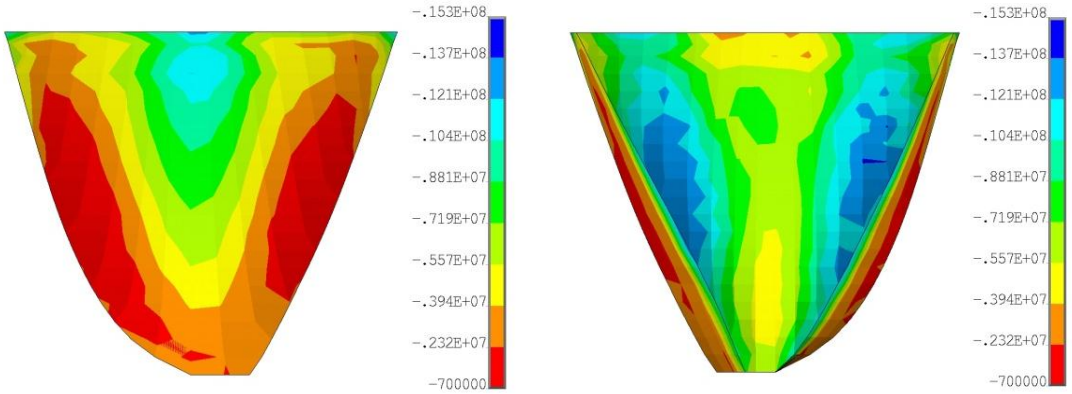

ETA20e-Average (DBL)

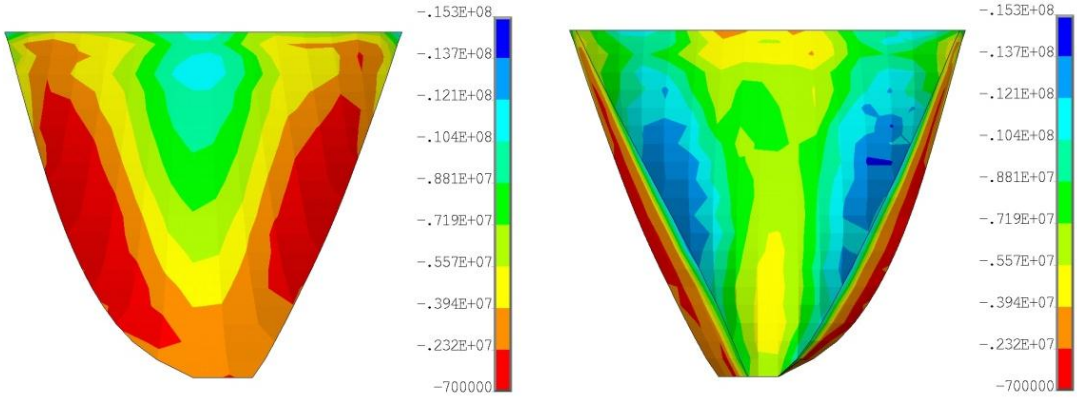

Accelerograms Average (DBL)

Figure 16. Average non-concurrent envelopes of S3 on US and DS faces; DBL

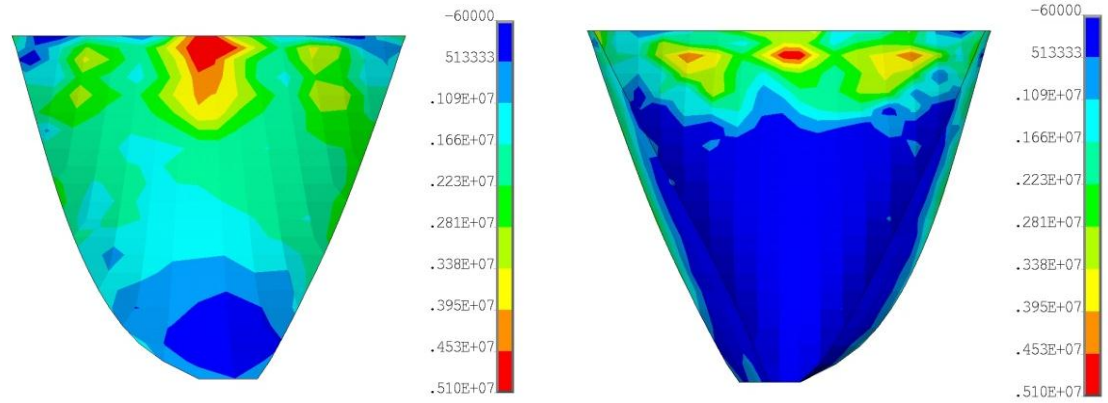

ETA20e-Average (MDL)

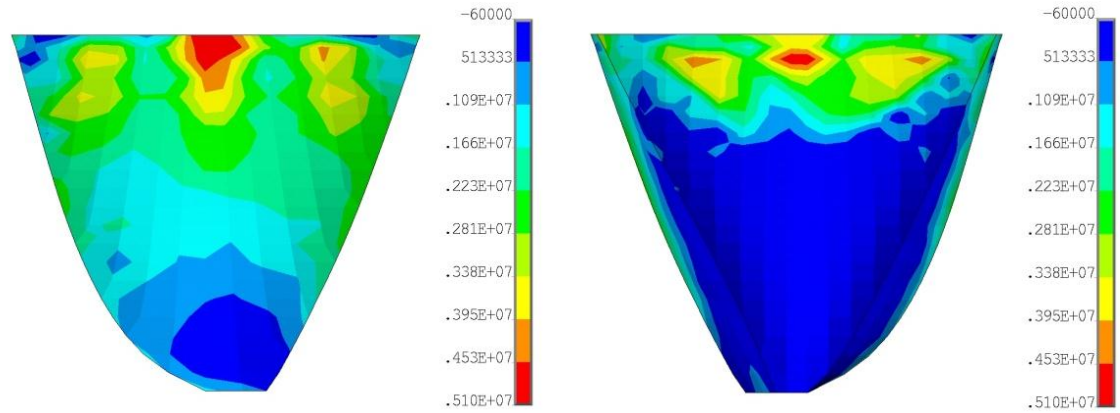

Accelerograms Average (MDL)

Figure 17. Average non-concurrent envelopes of S1 on US and DS faces; MDL

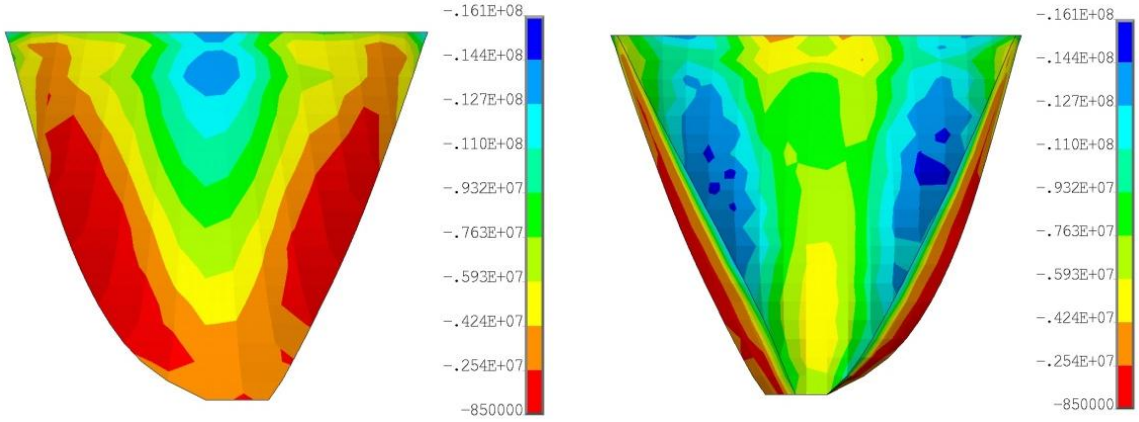

ETA20e-Average (MDL)

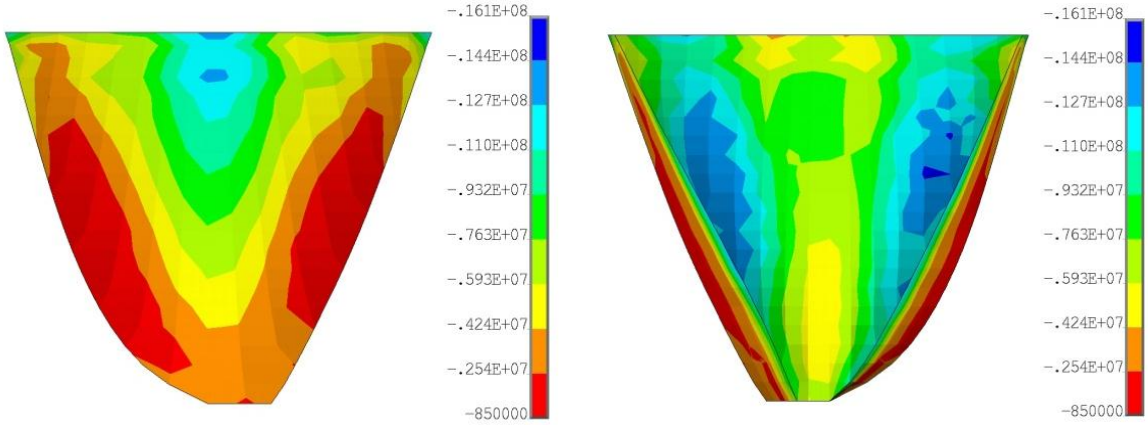

Accelerograms Average (MDL)

Figure 18. Average non-concurrent envelopes of S3 on US and DS faces; MDL

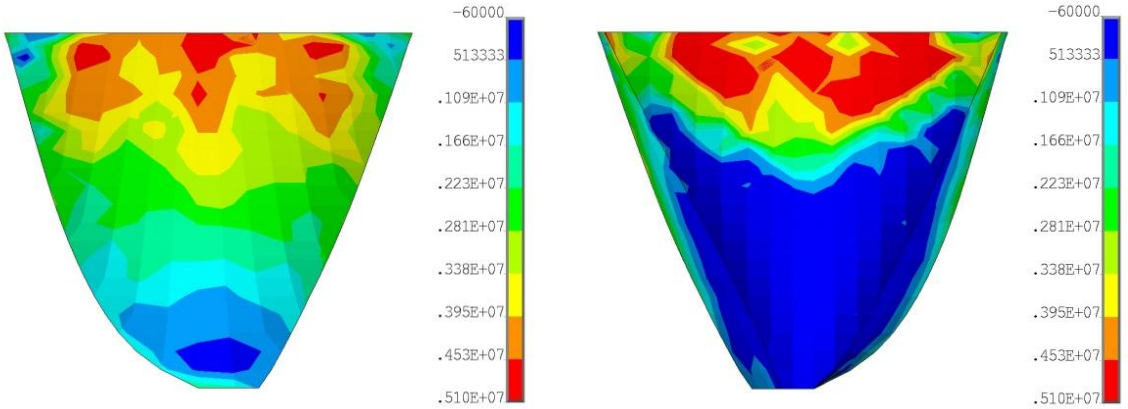

ETA20e-Average (MCL)

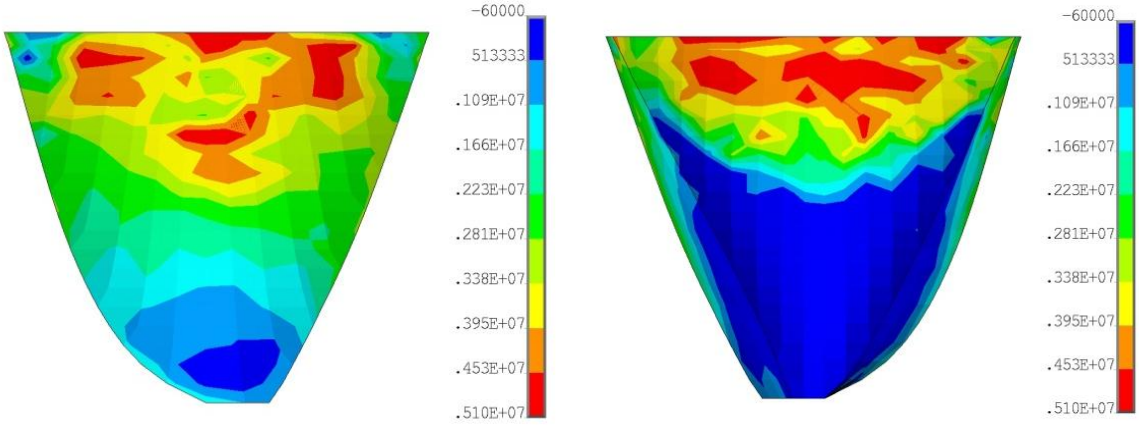

Accelerograms Average (MCL)

Figure 19. Average non-concurrent envelopes of S1 on US and DS faces; MCL

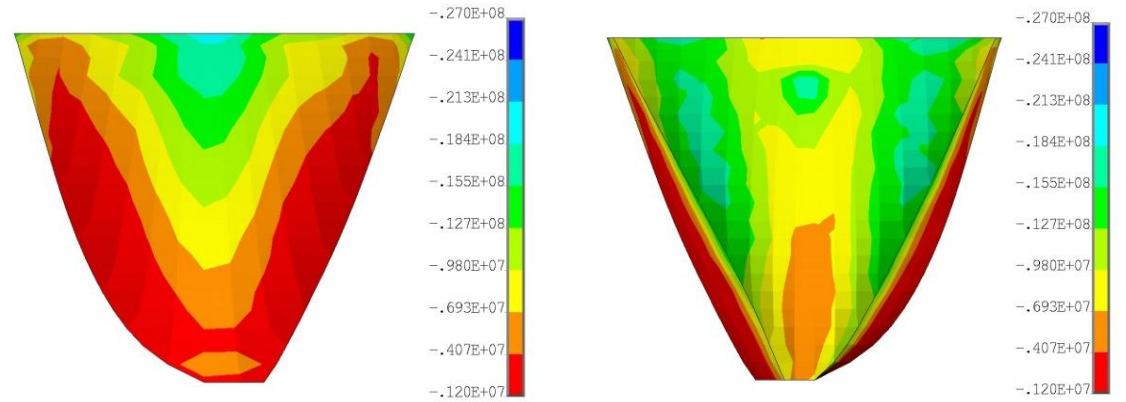

ETA20e-Average (MCL)

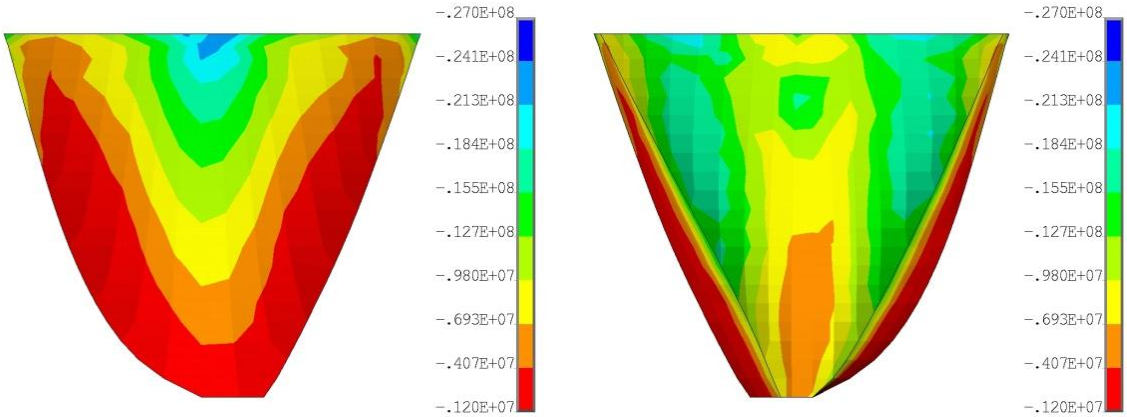

Accelerograms Average (MCL)

Figure 20. Average non-concurrent envelopes of S3 on US and DS faces; MCL

7.5. Crack profile

As mentioned before, cracking is simulated using smeared crack approach considering rotating crack model in which material is permitted to crack in three orthogonal directions. In addition to comparing various parameters obtained from ETA with THA results, it is necessary to study crack profiles caused by real accelerograms and ETAFs. It is worthy to note that there is no previously research on ability of ETA method in estimation of cumulative damage indexes like concrete cracking. Cumulative damage in the form of cracking usually occurs as result of ground motion intensity, pulse characteristics and sequencing, duration of shaking and other inherent characteristics of ground motion and in fact changes by ground motion itself. So estimation of real cracking behavior (especially in brittle material) not only is impossible under simulated ground motions but also it is very hard to find two ground motions in which produce same crack profile in structures under various performance levels. Considering the fact that all structure's responses is based on input energy to system and that the ETA method uses energy approach for matching response spectrum of ETAFs with accelerograms, so it is possible to compare crack profiles obtained from ETAFs and

accelerograms in each performance level. It is expected that ETAFs create similar crack profiles to those obtained from THAs in both location and extension. As it is obvious, ETAFs have always increasing demand in shaking duration and the decreasing part of real ground motions are not considered in these kinds of accelerograms, so probable propagation of cracks within dam body, as long as the shaking continues without increasing level of motion in real ground motions, are not happen in this case. Therefore it is possible to consider crack profiles generated by ETAFs as lower boundary of most critical crack profile under real ground motions.

Figure 21 shows cracked elements on US and DS faces of the dam created before dynamic analysis. These cracks which are in vicinity of PULVINO (concrete saddle) are due to implementing construction stages of the dam body, impounding reservoir and finallyapplying thermal loads.

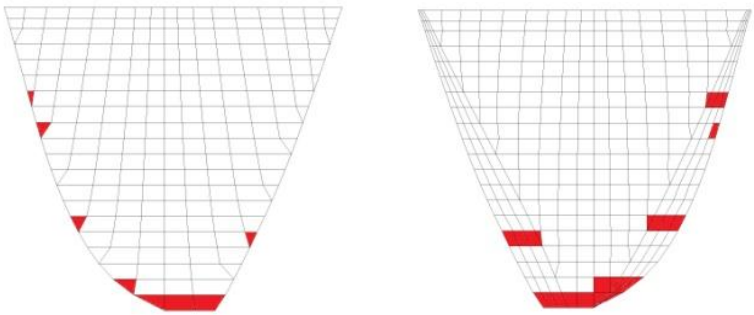

US face DS face

Figure 21. Cracked elements before dynamic analyses

Figure 22 and 23 show crack profiles in MCL extracted from TABAS and MANJIL accelerograms and three ETAFs until equivalent target time i.e. 6.36s for MCL. It is worthy to note that for each seismic input two series of profiles corresponding to +US/DS and –US/DS directions are plotted.

As can be seen, damage of the dam body (the number of cracked elements) under natural earthquakes is severe for MANJIL earthquake rather than TABAS. In addition, among ETAFs, ETA20e03 lead to more damage than the two others. Comparing the resulted crack profiles for a specific natural accelerogram shows differences in both the number of cracked elements and the crack pattern in the two opposite direction of excitations, so that one of these directions are critical in propagating crack within the dam body. Although there are differences in crack profiles resulted from ETAs in opposite directions, their profile are closer than accelerograms results. It is because of this fact that ETAFs are approximately symmetry with respect to the time axis. According to the Figures, it can be concluded that the ETAFs can predict the average crack profiles resulted from THAs corresponding to the MCL.

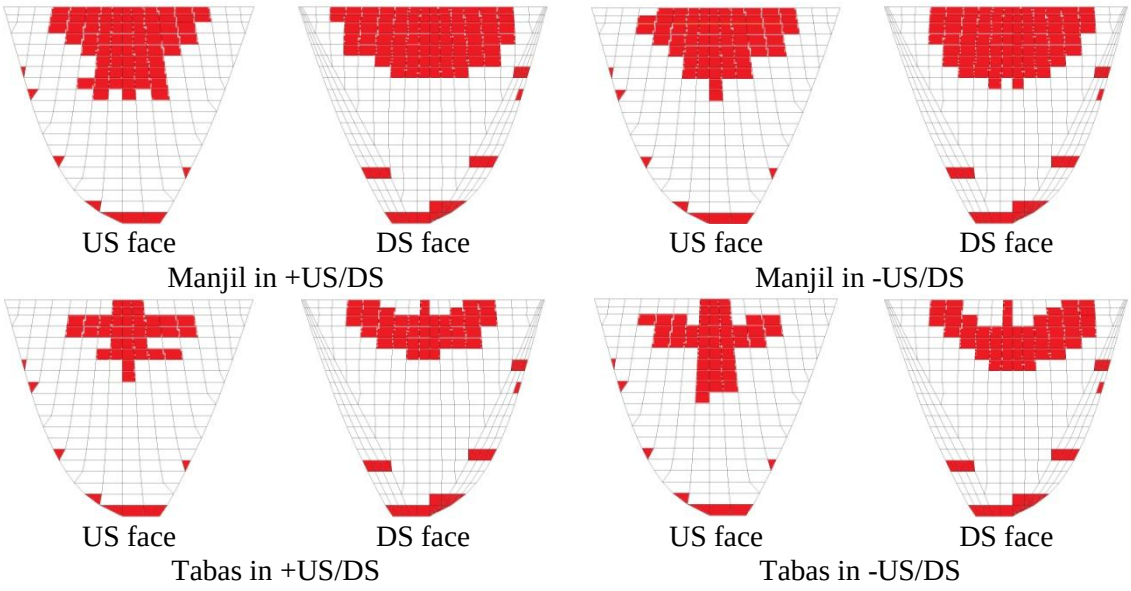

Figure 22. Cracked elements based on real accelerograms in MCL

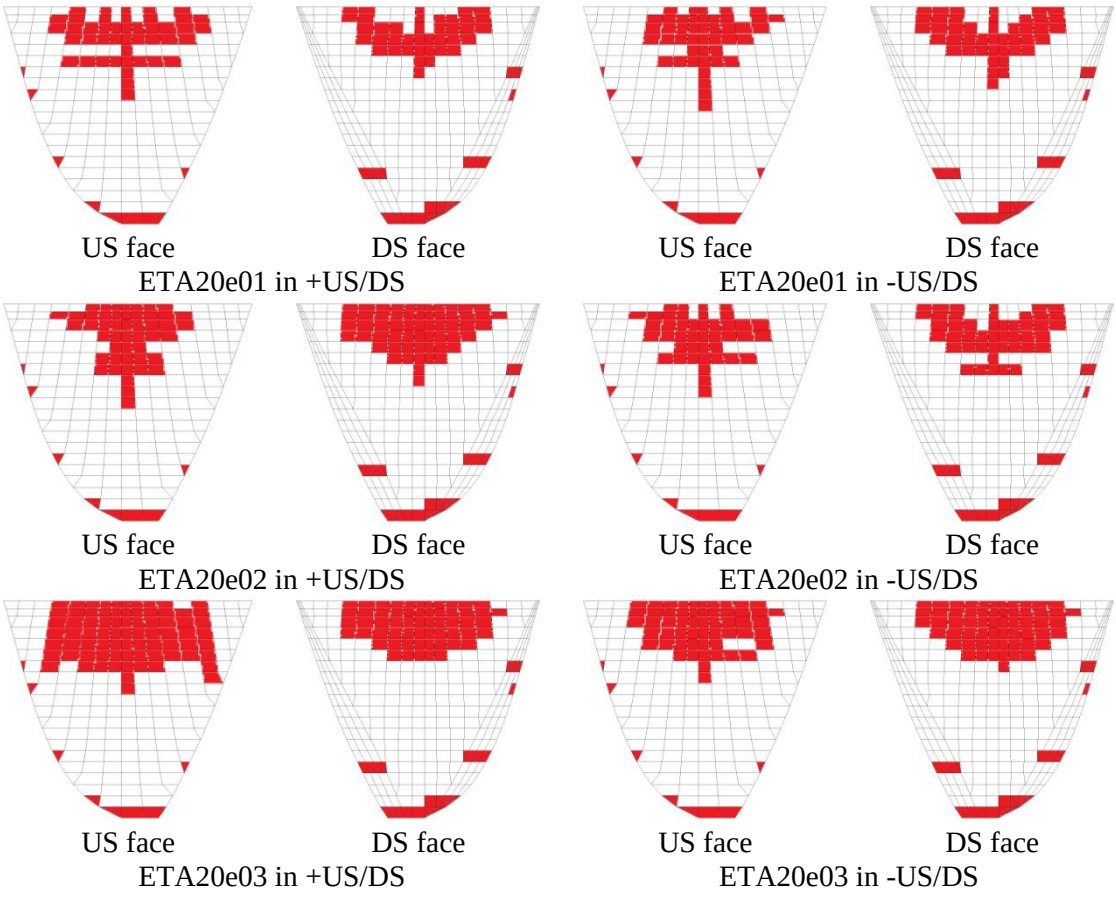

Figure 23. Cracked elements based on ETAFs up to equivalent target time for MCL

Figure 24 and Figure 25 show crack profile in MDL extracted from Loma-Prieta and Qaenaccelerograms and three ETAFs until equivalent target time for MDL which is 4.17s. It is clear that crack profiles are limited to some elements in central part of the dam in vicinity of the crest for all considered cases. The crack profile resulted from ETA20e01 is the same with Loma-Prieta in +US/DS direction. Also crack profiles resulted from ETA20e03 and Qaen in +US/DS direction are very similar. Finally, it can be concluded that ETA is capable to predict intensity and location of damaged areas in MDL with high accuracy.

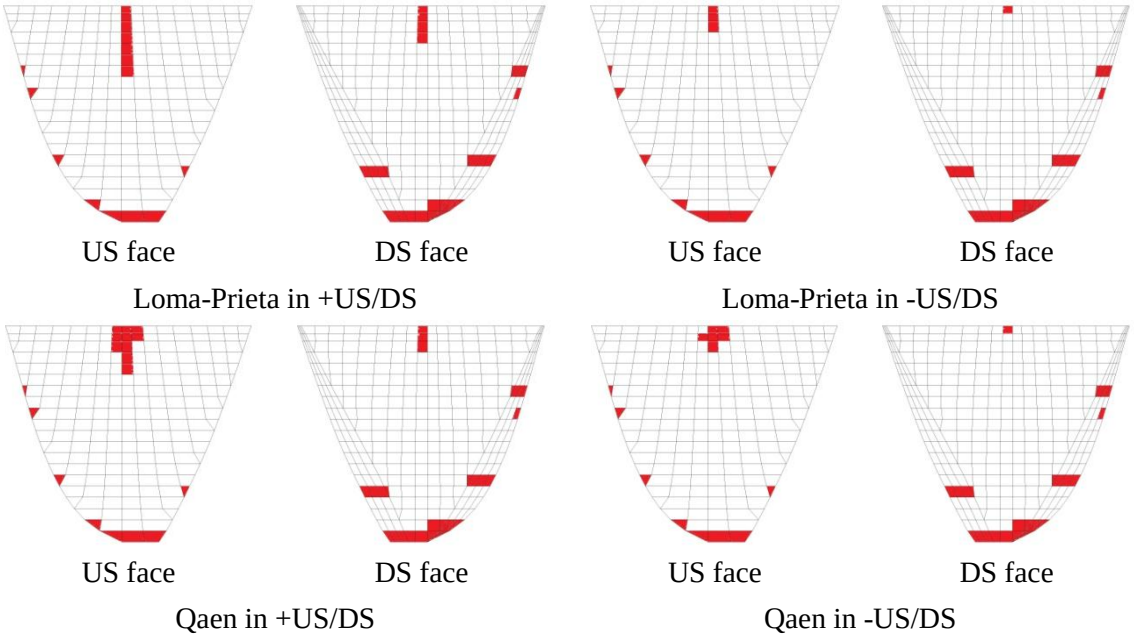

Figure 24. Cracked elements based on real accelerograms in MDL

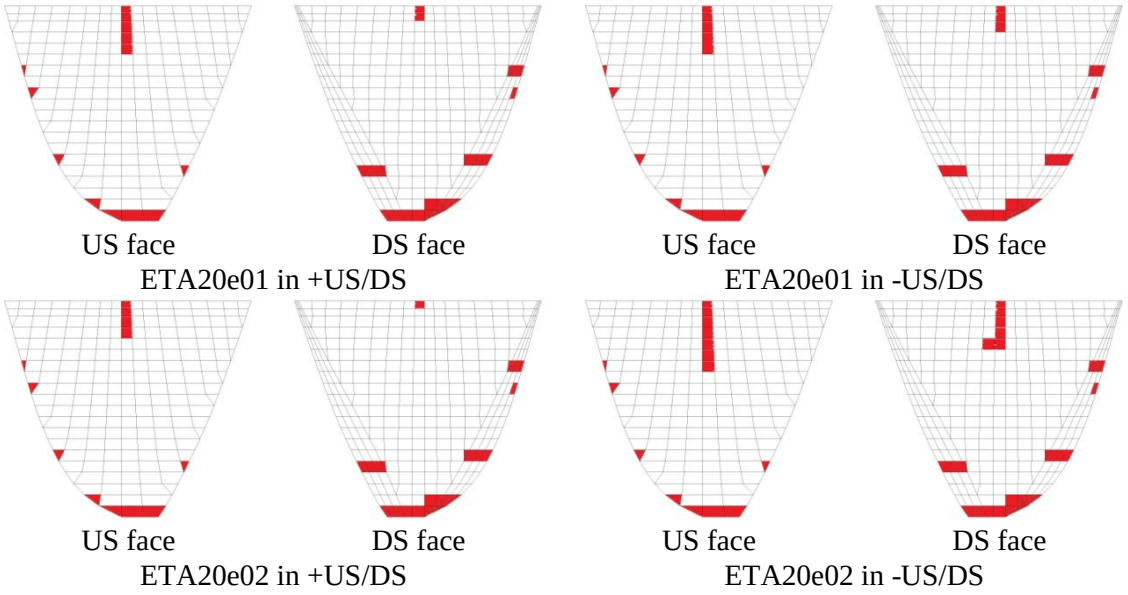

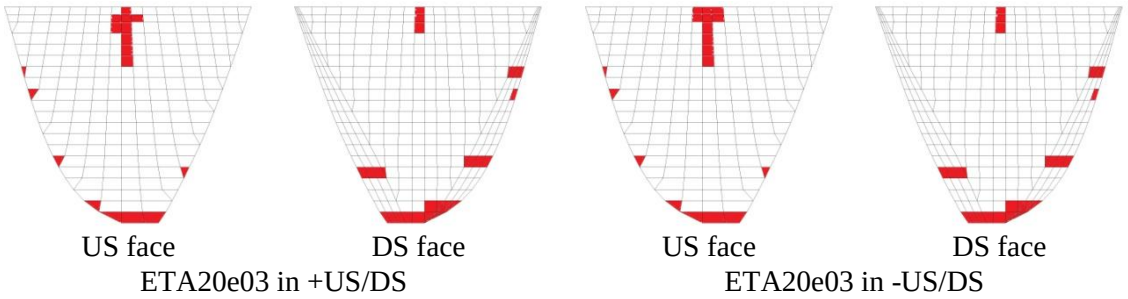

Figure 25. Cracked elements based on ETAFs up to equivalent target time for MDL

Figure 26 and 27 show crack profiles in DBL extracted from North-Ridge and Spitak accelerograms and three ETAFs until equivalent target time for MDL, 3.25s. As can be seen, no additional damages are created based on North-Ridge record in dam body. This is the same event based on ETA20e01. Moreover, two cracked elements are shown on US face of the dam based on Spitak and ETA20e02. It must be noticed that an additional cracked element is appear on DS face of the dam body based on ETA20e03 which is negligible.

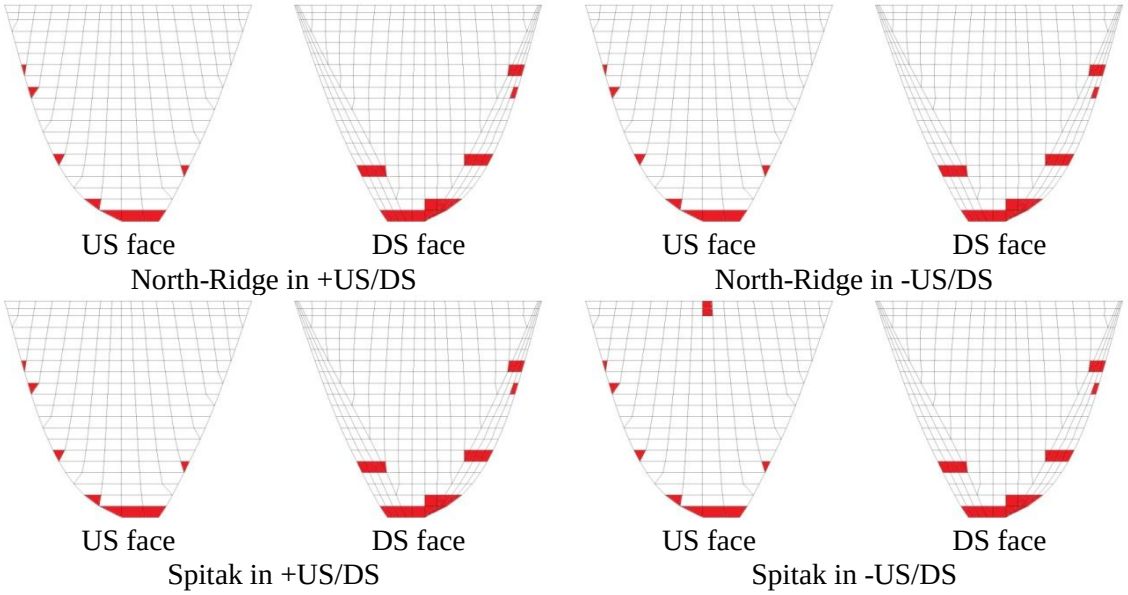

Figure 26. Cracked elements based on real accelerograms in DBL

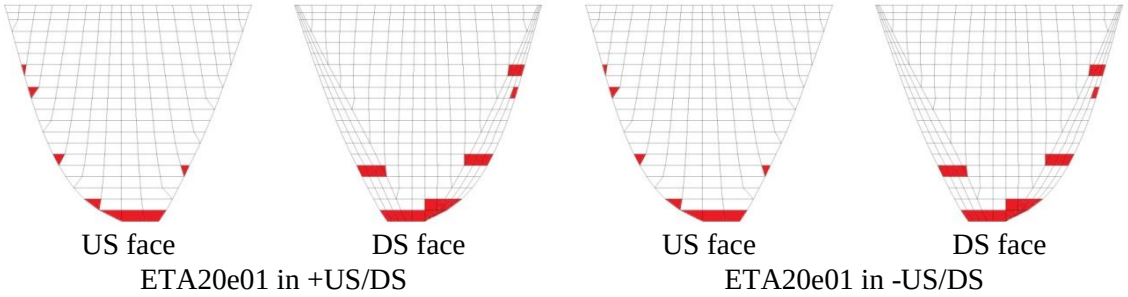

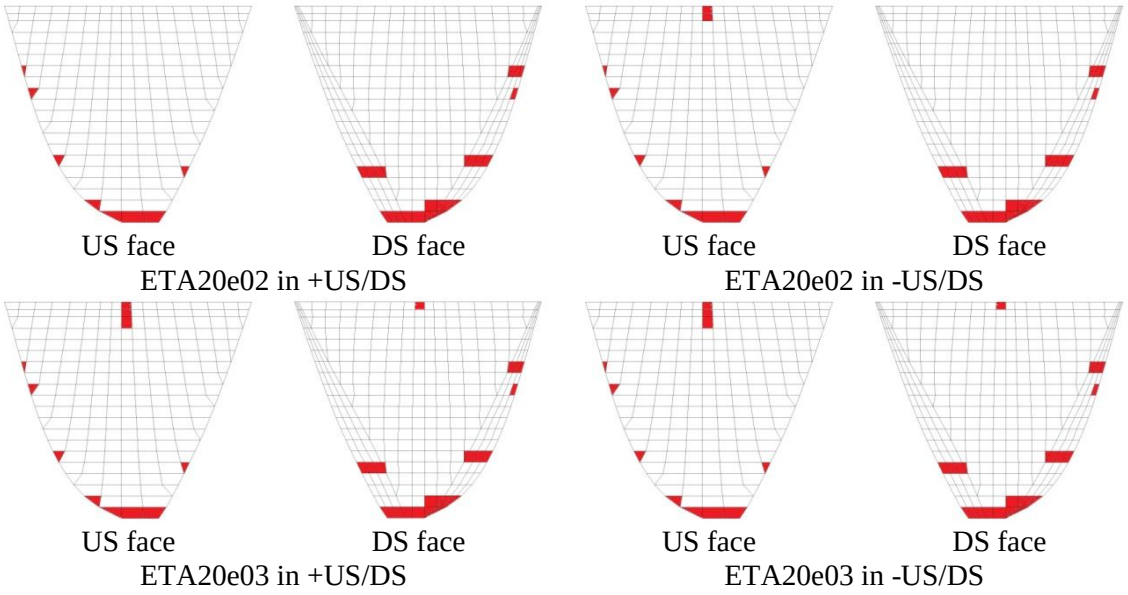

Figure 27. Cracked elements based on ETAFs up to equivalent target time for DBL

7.6. Discussion

Based on results obtained in previous subsections it is obvious that the system shows nonlinear behavior in higher seismic excitation levels in THAs. This is the same event in ETAs in higher seconds. Similarities of various responses between two methods are considerable in low and moderate seismic excitations and also in regions near the abutments. Increasing seismic performance level and considering the results in central upper part of dam (which shows severe oscillatory movement) shows some differences between ETA and THAs, but ETA completely is able to predict general trend of the response in all conditions.

Finally, the main advantage of ETA method lays on lower cost and time lapsing in comparison with several THAs required to obtain results in various performance levels. Figure 28shows total and selected duration for each of accelerograms used in TH analyses and ETAFs introduced in previous sections. Considering time step of 0.02s for accelerograms, the number of load steps required for analyses can be obtained by dividing selected duration to time step which is 16050 for total THAs.

On the other hand, referring to table2, it is obvious that the maximum target time which has been calculated for ETA is less than 7.00s (exactly 6.84s). So analyses of provided finite element model using first 7.00s of the three ETAFs in the two +US/DS and –US/DS directions lead to an analysis with total time of 42.00s. Considering that time step in ETAFs is 0.01s, the number of total load steps required for ETAs, is 4200.As can be seen, ETA reduces the total time and subsequently cost of analyses about 75% in comparison with THA method. Although the main time-consuming aspect of arch dam analysis is development of 3D model, analysis of such huge systems by various ground motions for reduction of dam responses dependency to selected ground motions can be a great concern for dam analyzers. On the other hand any probable changes in magnitude of ground motions

lead to total re-analysis of system, while in ETA method it is just needed to calculate new equivalent target time and evaluate results in this time without any more analysis.

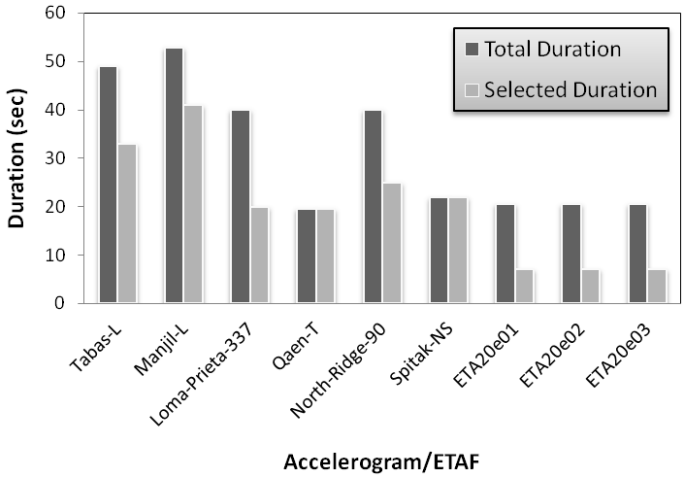

Figure 28. Total and selected duration for each of accelerograms and ETAFs in nonlinear analyses

8. CONCLUSION

At the present paper, Endurance Time Analysis method as a new time-history based dynamic pushover procedure was introduced and its application in nonlinear seismic analysis of concrete arch dam-reservoir-foundation system and also estimation of probable damages within dam body under real accelerograms was investigated. The reservoir water was supposed as compressible material and foundation rock was modelled as a mass-less medium to taking its flexibility during dynamic analyses. The β-Newmark time integration algorithm was used to solve the equation of motions in finite element model of dam-reservoir-foundation system. In static loading phase, the applied loads on the system were self weight, hydrostatic load in normal water level and thermal load corresponding to summer condition. All excitations in ETA and THA for the three performance levels (specified for the dam site) were applied in only one major direction (US/DS) considering two possible permutations.

Based on the conducted nonlinear dynamic analyses, it was found that all responses of the dam extracted from ETA up to the equivalent target time are in good agreement with the extreme values extracted from THAs. In addition, the general patterns of non-concurrent principal stress envelopes extracted from the two methods have similar appearance. Although percentages of errors are acceptable in lower excitation levels, some differences are observed in high excitation levels and for upper part of the dam body because the dam experiences sever damages in this region.

On the other hand, the profiles of cracked areas extracted from THAs were compared with those obtained from ETA up to the equivalent target time corresponding to each performance levels. The results prove that ETA method is able to estimate both location and

extension of cracked areas with reasonable accuracy. Generally, estimated cracked areas based on ETA are average of crack profiles generated from THAs in certain performance level in present study (and can assumed as lower boundary of the most critical crack profile which dam experience under specific performance level). Finally, the great advantage of ETA lays on low cost of analysis with respect to a set of THAs especially when the system should be analyzed in various performance levels. Considering benefit over cost theorem in analyzing dam-foundation-reservoir system using ETA shows that it has great ability to be used as alternative method for seismic evaluation of systems which includes a large number of elements like arch dams.

REFERENCES

1. Creager WP, Justin JD, Hinds J. *Engineering for Dams*, New York, John Wiley and Sons, Inc, 1964.
2. U.S. Bureau of Reclamation (USBR). *Design of Arch Dam*, U.S. Department of Interior, Denver Co, 1977.
3. Federal Energy Regulatory Commission Division of Dam Safety Inspection (FERC). Engineering guideline for the evaluation of hydropower projects-chapter 11: Arch dam design, USA, 1999.
4. Estekanchi HE, Vafai A, Sadeghazar M. Endurance time method for seismic analysis and design of structures, *Scientia Iranica*, 2004; **11**(4) 361–70.
5. Riahi HT, Estekanchi HE, and Vafai A. Endurance time method-application in nonlinear seismic analysis of single degree of freedom systems, *J Appl Sci*, 2009; **9**(10) 1817–32.
6. Estekanchi HE, Valamanesh V, Vafai A. Application of endurance time method in linear seismic analysis, *Eng Struct*, 2007; **29**(10) 2551–62.
7. Estekanchi HE, Riahi HT, and Vafai A. Endurance time method: exercise test applied to structures, *Asian J Civil Eng*, 2009; **10**(5) 559–77.
8. Estekanchi HE, Riahi HT, and Vafai A. Application of endurance time method in seismic assessment of steel frames, *Eng Struct*, 2011; **33**(9) 2535–46.
9. Hariri Ardebili MA, Zarringhalam Y, Yahyai M, Mirtaheri M. Nonlinear seismic response of steel concentrically braced frames using Endurance Time method, *Proceeding of 8th International Conference on Urban Earthquake Engineering (CUEE8)*, Tokyo, Japan, 2011.
10. Valamanesh V, Estekanchi HE. Endurance time method for multi-component analysis of steel elastic moment frames, *Scientia Iranica*, 2011; **18**(2) 139–49.
11. Alembagheri M, Estekanchi HE. Nonlinear analysis of aboveground anchored steel tanks using endurance time method, *Asian J Civil Eng*, 2011**; 12**(6) 731–50.
12. Alembagheri M, Estekanchi HE. Seismic assessment of unanchored steel storage tanks by endurance time method, *Earthquake Eng Vib*, 2011; **10**(4) 591–4.
13. Estekanchi HE, Alembagheri M. Seismic analysis of steel liquid storage tanks by endurance time method, *Thin-Walled Struct*, 2012; **50**(1) 14–23.
14. Tavazo M, Estekanchi HE, and Kaldi P. Endurance time method in the linear seismic

analysis of shell structures, *Int J Civil Eng*, 2012; **10**(3) 169–78.
15. Zeinoddini M, Nikoo HM, and Estekanchi HE. Endurance wave analysis (EWA) and its application for assessment of offshore structures under extreme waves, *Appl Ocean Res*, 2012; **37**, 98–110.
16. Valamanesh V, Estekanchi HE, Vafai A, Ghaemian M. Application of Endurance time method in seismic analysis of concrete gravity dams, *Scientia Iranica A*, 2011; **18**(3) 326–37.
17. Hariri Ardebili MA, Mirzabozorg H. Estimation of concrete arch dams responses in linear domain using endurance time analysis method, *J Civil Eng Architect*, 2011; **5**(8) 754–58.
18. Hariri Ardebili MA, Mirzabozorg H. Investigation of endurance time method capability in seismic performance evaluation of concrete arch dams, *J Dam Eng*, 2011; **XXII**(1) 35–64.
19. Hariri Ardebili MA, Mirzabozorg H, and Estekanchi HE. Capability of endurance time method in analysis of arch dams and prediction of joints behavior, *Proceeding of the 6th International Conference in Dam Engineering*, Lisbon, Portugal, 2011.
20. Estekanchi HE, Arjomandi K, Vafai A. Estimating structural damage of steel moment frames by endurance time method, *J Construct Steel Res*, **64**(2) (2008) 145-55.
21. U.S. Army Corps of Engineering (USACE). EM 1110-2-6053: Earthquake design and evaluation of concrete hydraulic structures, Washington D.C., USA, 2007.
22. Clough RW, Penzien J. *Dynamics of Structures*, McGraw-Hill Inc, London, UK, 1993.
23. Building and Housing Research Center (BHRC), Iranian code of practice for seismic resistant design of buildings, standard No. 2800-05, Tehran, Iran, 3rd edition, 2005.
24. Estekanchi HE, Valamanesh V, and Vafai A. Characteristics of second generation endurance time acceleration functions, *Scientia Iranica*, 2010; **17**(1) 53–61.
25. Nozari A, Estekanchi HE. Optimization of endurance time acceleration functions for seismic assessment of structures, *Int J Optim Civil Eng*, 2011; **1**(2) 257–77.
26. Sheibany F, Ghaemian M. Effects of environmental action on thermal stress analysis of Karaj concrete arch dam, *ASCE J Eng Mech*, 2006; **132**(5) 532–44.
27. Valamanesh V, Estekanchi HE. A study of endurance time method in the analysis of elastic moment frames under three-directional seismic loading, *AJCE*, 2006; **11**(5) 543–62.
28. International Committee on Large Dams (ICOLD), *Selecting Seismic Parameters for Large Dams*, ICOLD Bulletin, 1989; **72**, 11-31.
29. Behan-sad Engineering and Consulting Co. *Seismic hazard analysis of DEZ dam*, Tehran, Iran, 2009.
30. Hariri Ardebili MA, Mirzabozorg H, Ghaemian M, Akhavan M, and Amini R. Calibration of 3D FE model of DEZ high arch dam in thermal and static conditions using instruments and site observation, *Proceedings of 6th International Conference in Dam Engineering*, Lisbon, Portugal, 2011.
31. Hariri Ardebili MA, Mirzabozorg H. Seismic Performance Evaluation and Analysis of Major Arch Dams Considering Material and Joint Nonlinearity Effects, *ISRN Civil Engineering*, Vol. 2012, Article ID 681350, 10 pages, doi:10.5402/2012/681350.
32. Gunn RM. Non-linear design and safety analysis of arch dams using damage

mechanics; Part I: formulation, *Hydropower and Dams*, 2001; **2**, 67–74.
33. Hariri Ardebili MA, Kolbadi SM, Heshmati M, and Mirzabozorg M. Nonlinear analysis of concrete structural components using co-axial rotating smeared crack model, *J Appl Sci*, 2012; **12**(3) 221–32.